

# Aerial Intelligent Reflecting Surfaces in MIMO-NOMA Networks: Fundamentals, Potential Achievements, and Challenges

BRENA KELLY S. LIMA<sup>1</sup>, ARTHUR SOUSA DE SENA<sup>2</sup>, RUI DINIS<sup>5</sup> (Senior Member, IEEE), DANIEL BENEVIDES DA COSTA<sup>4</sup> (Senior Member, IEEE), MARKO BEKO<sup>1,5</sup>, RODOLFO OLIVEIRA<sup>3,5</sup> (Senior Member, IEEE), AND MÉROUANE DEBBAH<sup>4</sup> (Fellow, IEEE)

<sup>1</sup>COPELABS, Lusofona University, 1749-024 Lisbon, Portugal

<sup>2</sup>Department of Electrical Engineering, Lappeenranta-Lahti University of Technology, 53850 Lappeenranta, Finland

<sup>3</sup>Departamento de Engenharia Electrotécnica e de Computadores, Faculdade de Ciências e Tecnologia, Universidade Nova de Lisboa, 2829-516 Caparica, Portugal

<sup>4</sup>Digital Science Research Center, Technology Innovation Institute, Abu Dhabi, UAE

<sup>5</sup>Instituto de Telecomunicações, Instituto Superior Técnico, University of Lisbon, 1649-004 Lisbon, Portugal

CORRESPONDING AUTHOR: D. B. DA COSTA (e-mail: danielbcosta@ieee.org)

This work was supported by the Fundação para a Ciência e Tecnologia through the IT Project under Grant UIDB/50008/2020.

**ABSTRACT** Non-orthogonal multiple access (NOMA) technique and unmanned aerial vehicles (UAVs) have been recognized as promising technologies for enabling the stringent requirements of the different network infrastructures expected for the next generation of wireless networks. In parallel, intelligent reconfigurable surfaces (IRSs) have been widely pointed out as an auspicious solution to further improve spectral efficiency, coverage range, and connectivity. By integrating IRS with UAV and NOMA schemes with multiple-input multiple-output (MIMO) it is possible to smartly improve the overall network performance. In order to explore some of these potentials, this paper provides a comprehensive discussion about the interplay of aerial IRS in MIMO-NOMA (AIRS-NOMA) networks, as well its architecture, functionality principles, and performance gains. In particular, attractive gains related to the data rate maximization, user fairness, energy efficiency, and coverage range are highlighted. Simulation results are provided to support our insightful discussions, in which it is revealed that the performance gains of AIRS-NOMA networks are superior when compared to terrestrial deployment. In addition, to guide new studies perspectives, it is addressed some issues and research opportunities associated with this potential integration.

**INDEX TERMS** Intelligent reflecting surface (IRS), multiple-input multiple-output (MIMO), non-orthogonal multiple access (NOMA), unmanned aerial vehicle (UAV).

## I. INTRODUCTION

THE NUMBER of connected devices across the world has been foreseen to surpass 75.4 billion by 2025 [1]. This number is related to the diverse services and applications expected for sixth-generation (6G) wireless systems, ranging from smart homes and self-driving cars to interconnected low-power sensors in health, factories, and agriculture. These different network infrastructures will

impose stringent requirements to system designers, such as reliable communications, massive connectivity, low latency, low energy consumption, seamless connectivity, and high spectral efficiency. To achieve these heterogeneous requisites, numerous strategies and transmission technologies have been proposed.

The design of appropriate multiple access techniques is crucial for supporting the massive number of devices

foreseen for future networks. In particular, non-orthogonal multiple access (NOMA) has been regarded as a promising candidate technique for next-generation wireless networks due to its potential in achieving high spectral efficiency, massive connectivity, low latency, and user fairness, which can outperform orthogonal multiple access counterparts [2]. By performing superposition coding (SC) at the transmitter and successive interference cancellation (SIC) at the receiver, power-domain NOMA enables multiple users to share the same resource block with distinct power levels [3].

In parallel, unmanned aerial vehicles (UAVs) working as aerial base stations (BSs) have also been identified as enablers of future-generation wireless networks due to their attractive characteristics, such as the ability to perform complex tasks in diverse scenarios and the flexible configuration and deployment in comparison with ground BS. Due to these features, UAVs can significantly improve the connectivity and coverage range of communication networks, therefore, reducing the need for deploying expensive towers [4]. Unlike terrestrial BSs, the channels between UAV and ground devices have a high probability of being dominated by line-of-sight (LoS) links, which can provide significant performance improvement for the communication system.

In order to improve the propagation environment and enhancing the signal strength of 6G systems, intelligent reflecting surfaces (IRSs) have arisen as another promising technology. An IRS is a planar metasurface composed of a large number of reflecting elements that can be controlled via integrated electronics [5]. In general, IRS structures are composed of nearly passive elements that can significantly reduce energy consumption [6]. Thus, IRSs can be more energy-efficient than conventional relaying strategies. Moreover, each reflecting element can be programmed independently to induce distinct phase and amplitude changes, which enables IRSs to reflect and steer impinging waves, ideally, towards any desired direction. This feature, commonly called passive beamforming, can maximize effective channel gains and enhance the reliability of received signals. Signal beams can be formed to weaken the interference coming from non-desirable devices or to avoid information leakage. In the deployment context, the intrinsic features of IRS can be efficiently integrated with other emerging technologies in order to achieve enormous gains for the overall network [7]–[10]. Next, we present a comprehensive state-of-the-art related to the IRS technology.

#### A. STATE-OF-THE-ART

Despite such promising opportunities for the combination of UAV, NOMA and IRS technologies, one must address several technical challenges to effectively use them for each specific networking application. To tackle these problems and challenges, research efforts are being carried out in the context of these technologies. Based on this, a descriptive state-of-the-art of the IRS, UAV, and NOMA techniques is presented as follows.

#### 1) AERIAL IRS

In recent years, numerous works have been developed in the field of IRS-mounted on the UAV to demonstrate their role in improving network performance, explore the feasibility of building a controllable and programmable radio environment, and to corroborate the compatibility of deployment with technologies already existing. More specifically, in these papers, the integration of IRS on aerial platforms has been extensively investigated due to the numerous benefits compared to terrestrial IRS (TIRS) designs, among them flexible deployment and full-angle panoramic reflection ( $360^\circ$ ). Moreover, in aerial IRS (AIRS) only one reflection is sufficient due to LoS, while for terrestrial designs multiple reflections are required due to non line-of-sight (NLoS), which makes the TIRS design relatively large to improve beam propagation. Due to the numerous benefits compared to TIRS, AIRS is a research topic with a wide potential. In particular, a comprehensive overview of the combination of UAV and IRS in [11], where two case studies were carried out to optimize the UAV trajectory, the transmit beamforming, and the IRS passive beamforming. Types of aerial platforms, their operation, control architecture, and types of communication were investigated in [12]. The joint optimization of phase shifts, placement, and passive beamforming for the AIRS was considered in [13] and [14] to maximize the worst-case signal-to-noise ratio.

When multiple UAVs are deployed to enable AIRS communication, numerous applications and challenges can be explored. In [15], the authors investigated multiple UAVs cooperatively. The authors presented an overview of the UAV swarm-enabled AIRS, including its motivations and competitive advantages compared to terrestrial and aerial IRS, as well as its applications and challenges of designing in wireless networks. In [16], methods to improve the coverage of served users by multiple AIRS were introduced, and the maximum achievable coverage probabilities of the two users were derived and analyzed.

By considering a more realistic modeling channel, where communication systems were characterized by Nakagami- $m$  small-scale fading and inverse-Gamma large scale shadowing, in [17] the authors investigated the delay-limited performance and the outage probability. On the other hand, the compatibility and feasibility of AIRS in a cell-free massive multiple-input multiple-output (MIMO) network to maximize the user's achievable rate were investigated in [18]. In [19], the authors investigated AIRS to support ultra-reliable low latency (URLLC) communication to tackle the interference caused by the dense network. An AIRS communication system over Terahertz (THz) bands for confidential data dissemination from an access point (AP) towards multiple ground user equipments (UEs) on the Internet-of-Things (IoT) networks was investigated in [20]. In order to analyze the performance of AIRS under high-altitude, a wireless architecture mounted on a high-altitude aerial platform enabled by AIRS was investigated in [21]. The placement and array-partition strategies

of aerial-IRS and the phases of IRS elements were jointly optimized. In addition, resource management for transmit power minimization in AIRS HetNets supported by dual connectivity was investigated in [22]. The authors studied the problem of total transmit power minimization by jointly optimizing the trajectory/velocity of each UAV, IRSs' phase shifts, subcarrier allocations, and active beamformers at each BS.

## 2) UAV WITH TERRESTRIAL IRS

The terrestrial IRS, commonly mounted in building facade, ceilings, and furniture, in UAV-enabled wireless networks have been explored in numerous scientific works [23]–[31]. In [23], the authors investigated the coverage IRS-assisted transmission strategy to support multi-user. A transmission protocol was proposed to adjust the transmission strategy for all UAV-user pairs by addressing the IRS elements' allocation and their phase shifts configuration. In order to maximize the sum rate of the network, in [24] the authors investigated multiple UAVs acting as aerial BS employing NOMA to serve multiple groups. The reflection matrix of the IRS and the NOMA decoding orders among users were optimized. On the other hand, to maximize the achievable rate, the UAV trajectory and IRS's passive beamforming design were optimized in [25].

In order to maximize the network's throughput by jointly optimizing the UAV's trajectory, IoT's energy harvesting time scheduling, and the phase shift matrix, a simultaneous wireless power transfer and information transmission (SWIPT) scheme for IoT devices with support from IRS-aided UAV communication was investigated in [26]. In the same direction, the authors in [27] studied IRS-assisted UAV for timely data collection in IoT networks. The phase shift of IRS elements, the scheduling of IoT devices transmissions, and the trajectory of the UAV were optimized to maximize the total number of served devices. To minimize the energy consumption, the integration of IRS into UAV-NOMA systems by jointly designing the movement of the UAV, phase shifts of the IRS, power allocation policy at the UAV, and the decoding order was investigated in [28].

To solve the continuous optimization problem with time-varying channels in a centralized fashion, the joint optimization of the power allocation and the phase-shift matrix of a IRS-assisted multi-UAV network was investigated in [29]. Under the presence of multiple nonidentical interference links, the authors in [30] investigated IRS-assisted UAV-enabled vehicular communication systems with infinite and finite blocklength codes. On the other hand, a IRS-assisted UAV physical-layer secure communication for improving the system secrecy rate was investigated in [31] in order to maximize the average worst-case secrecy rate.

## 3) TERRESTRIAL IRS WITH NOMA

A comprehensive overview of the recent progress on the integration of TIRSs and NOMA was presented in [32]

and [33]. The fundamentals of the two techniques were introduced, and then the basic concepts of the integration of the IRSs and NOMA were discussed. In parallel, in [34] was presented a comprehensive discussion of the role of TIRS in MIMO-NOMA systems. Attractive performance gains to the communication networks were identified, such as higher data rates, improved user fairness, and possibly higher energy efficiency. In [35], the authors optimized the rate performance of the IRS-assisted NOMA system, while ensuring user fairness. By jointly optimizing the active transmit beamforming at the BS and passive beamforming at the IRS, the authors considered the maximizing of the minimum decoding signal-to-interference-plus-noise-ratio (SINR) of all users.

In [36], the authors investigated both downlink and uplink IRS-NOMA network. On the other hand, in [37] the authors investigated an IRS-assisted NOMA downlink system under both continuous and discrete phase-shifting IRS. Then, closed-form expressions for the average required to transmit power, the outage probability, and the diversity order were derived. User pairing and fixed power allocation scheme to enable RIS-NOMA network were investigated in [38]. To explore the IRS-NOMA network with residual hardware impairment (RHI) in IoT scenarios, the impact of RHI on the physical layer security performance was investigated in [39]. IRS-enabled MIMO-NOMA networks were investigated in [40] and [41]. More specifically, in [40] a dual-polarized IRS was investigated to improve the performance of dual-polarized massive MIMO-NOMA networks. The proposed scheme alleviates the impact of imperfect SIC and enables users to exploit polarization diversity with near-zero inter-subset interference. On the other hand, a passive beamforming weight at IRS in a MIMO-NOMA network was proposed in [41]. The channel statistics, outage probability, ergodic rate, spectral efficiency, and energy efficiency were derived in closed-form expressions.

## 4) MACHINE LEARNING IN AIRS-NOMA NETWORKS

In an effort to effectively exploit IRSs for optimizing wireless systems, solutions based on machine learning methods have been investigated along of the years. In [42], the authors introduced machine learning for user partitioning and phase shifters design in IRS-aided NOMA networks. On the other hand, the authors in [43] explored THz massive MIMO-NOMA with IRS and proposed a smart reconfigurable scheme, which can realize customizable and intelligent communications by flexibly and coordinately reconfiguring hybrid beams through the cooperation between access points and IRS.

In particular, deep reinforcement learning (DRL) and reinforcement learning (RL) algorithms, branches of machine learning, have been proposed and applied to solve different problems related to IRS-enabled communication systems. In [44], the authors investigated a single-antenna transmission of IRS-assisted NOMA network and two RL algorithms were proposed to solve the problem caused by the overhead. In [45], two RL-based algorithms were adopted to

**TABLE 1.** List of the papers that considered the integration of IRS in future wireless technologies, such as UAV, NOMA, and MIMO. Notions: ✓ → partial discussion. ✓✓ → Detailed discussion. x → no discussion. \* → text-based work. \*\* → text- and performance-based work.

References	Type	AIRS	TIRS	NOMA	MIMO
[5], [6]	*	x	✓✓	x	x
[7]	*	✓	✓✓	✓	✓
[8], [9]	*	x	✓✓	✓	✓
[10]	*	✓✓	x	✓	x
[11]	**	✓✓	✓	x	x
[12], [15]	**	✓✓	x	x	x
[32]	**	✓	✓✓	✓✓	✓
[33]	*	x	✓✓	✓✓	x
[34]	**	x	✓✓	✓✓	✓✓
[56]	**	x	✓✓	✓	x
[59]	*	✓	✓✓	✓	x
Our paper	**	✓✓	✓	✓✓	✓✓

solve a resource allocation problem in order to minimize the average age-of-information of the users in IoT networks. The freshness of collected data of the IoT devices was improved via optimizing power, sub-carrier, trajectory variables, and the phase shift matrix elements. In [46], the authors investigated an IRS-aided multi-robot served by an AP through the NOMA technique. A dueling double deep Q-network-based algorithm was used to jointly optimize the trajectories, decoding orders, reflecting coefficients, and the power allocation of the AP.

In [47], the authors investigated the application of deep deterministic policy gradient to the AIRS-NOMA network with multiple users. The power allocation of the BS, the phase shifting of the IRS, and the horizontal position of the UAV were jointly optimized. In [48], the authors investigated a DRL-based relay selection scheme for cooperative networks with IRS. A DRL-based framework was proposed in [49] to jointly optimize the IRS and reader beamforming, with no knowledge of the channels or ambient signal in an ambient backscatter communications system aided by an IRS. In [50], the authors investigated a UAV-powered IoT network. A multi-agent DRL approach was proposed to find the optimal collaboration strategy of these energy-limited UAVs that maximizes the accumulated throughput of the IoT network. In [51], a three-step approach based on machine learning was proposed to maximize the sum-rate of all users in a TIRS-aided multiple-input single-output (MISO)-NOMA network by jointly optimizing the passive beamforming of the IRS, decoding order, and power coefficient allocation, subject to the rate requirements of users.

In order to summarise the main papers presented in this work, Table 1 presents a list of works that considered the integration of IRS, UAV, NOMA, and MIMO.

## B. MOTIVATION AND CONTRIBUTIONS

Although there is substantial work on AIRS, MIMO and NOMA networks, there are no works that specifically incorporate AIRS in MIMO-NOMA networks, demonstrating the

role of this interaction in terms of its potential achievements. Inspired by the aforementioned considerations, it is provided a comprehensive discussion based on performance analysis related to the AIRS-NOMA networks in order to show the potential improvements and new insights that can be attained due to this promising integration. In particular, the features of the paper refers to the timeliness and importance of the research topic, and the lack of works in the current literature providing discerning discussions, from an informative guide perspective, on the considered scenario. To provide a consistent guide, the fundamental principles of IRS and its integration into aerial platforms are introduced and, then, the system model of AIRS-NOMA network is presented. Once the system model has been detailed, it is discussed the potential realizations that AIRS-NOMA systems are capable of offering, where numerical simulations are presented to demonstrate the achieved performance gain when this setup is employed. The attained results show that this strategy achieves satisfactory results in terms of achievable rate, user fairness, energy efficiency, and coverage area when compared to the terrestrial IRS MIMO-NOMA (TIRS-NOMA), and aerial decode-and-forward relaying with NOMA (ADF-NOMA) scheme. Furthermore, characteristics of this design are highlighted, as well potential scenarios, research challenges to inspire future research, and solutions for the design and implementation of AIRS-NOMA networks.

The remainder of this paper is organized as follows. Section II describes the fundamentals of AIRS-NOMA technology and the system model under consideration. Section III presents the potential achievement of the integration of AIRS-NOMA system in comparison with terrestrial deployment. In Section IV, we conduct a discussion about research opportunities associated with the integration of AIRS-NOMA networks. Finally, the conclusions are presented in Section V.

## II. FUNDAMENTALS OF AIRS AND MIMO-NOMA

In this section, we provide a background of the IRS hardware and the control architecture of the IRS mounted on UAV.

### A. PRINCIPLES OF IRS STRUCTURE

Motivated by recent advances in the field of electromagnetic (EM) materials, IRS frameworks are envisioned as a revolutionary solution for the next generation of wireless communication. IRS is a planar meta-surface made of a large number of low-cost and passive meta-materials. The meta-surface structure is composed of ultra-thin layers of different EM elements, also known as meta-atoms. The key feature of the IRS structure is that each meta-atom can modify the impinging waves in ways that conventional materials cannot. In particular, each meta-atom can be configured in real-time with different phases and amplitudes to dynamically adapt to the fluctuations/characteristics of the environment and reflect the signal in the desired direction. In general, an IRS architecture is composed of at least three layers. The first layer

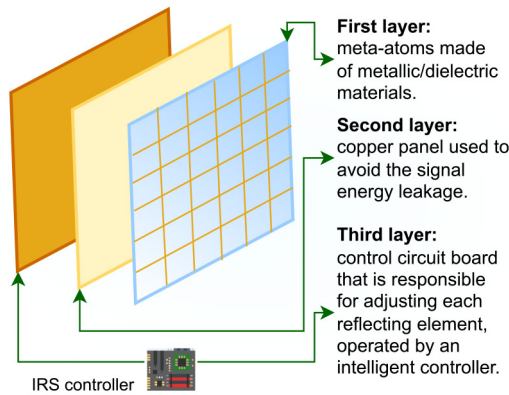


FIGURE 1. Illustration of the IRS structure.

consists of a large number of meta-atoms made of metallic/dielectric materials, which act directly in the process of reflecting the signal. The second layer consists of a copper panel to avoid signal/power leakage. The third layer, also called the control layer, consists of an electronic board composed of circuits capable of controlling the reflection coefficients (amplitude/phase shift) of each meta-atom, and it is operated by an intelligent controller. In addition, this layer can also act as a gateway to communicate and coordinate with other network components. In order to summarize the aforementioned layers, a generic IRS structure is illustrated in Fig. 1.

Unlike structures composed of active materials, a passive metasurface does not require high-energy consumption, complex circuits, and expensive materials [7]. It is noteworthy that, naturally, IRSs support advanced wireless waveforms and operate in full-duplex mode without generating self-interference and noise amplification. In consequence, the IRS framework does not require complex processing to encode and decode the information, which significantly minimizes power consumption and complexity when compared to conventional technologies, such as MIMO beamforming and relaying systems, i.e., decode-and-forward (DF) and amplify-and-forward (AF).

### B. ARCHITECTURE OF AIRS

UAVs have been widely used to enhance network performance. Then, the design and benefits of UAVs as aerial BSs in a wireless network were explored in numerous researches [4]. When IRSs are employed in an aerial platform, it is possible to achieve significant performance improvement to the network due to the high flexibility/mobility that UAVs can provide. In addition, if the LoS links between the BS and UAV, and/or UAV and users are blocked by obstacles, the reflecting elements can be accurately adjusted to form virtual LoS links. This solution is one alternative to enhance the coverage area, throughput and capacity both in urban environments and in remote areas,

without expensive implementation cost. In particular, a typical control architecture of UAV equipped with IRS can be summarized as follows:

- Terrestrial control: it consists of a processing central composed of radio-frequency transmitters capable of analyzing the environment data, management trajectory information, and communication tasks. Once the metasurface reflector is made of passive elements, the IRSs do not employ processing functions. Then, the terrestrial unit is responsible to process the sensed data, providing the channel state information (CSI) and the angle of arrival (AoA) between the UAV and users. It is noteworthy that the tasks to obtain data about channel modeling and estimation in the IRS-enhanced UAV networks are extremely difficult due to the dynamic nature of the system. This interesting topic arises as promising research possibilities and will be in-depth explored in challenges and research opportunities in this work.
- UAV Control: it consists of an aerial onboard coupled to the UAV to perform flight and IRS control. Given a set of environment conditions, it is possible to improve the mobility and establishment of the UAV. This unit performs the management of the battery, communication gateway, and arrangement of reflecting elements of the meta-surface. The meta-surface coupled to the UAV can be designed in three-layers, as aforementioned. In addition, the UAV control unit can send and receive pilot symbols to the terrestrial control unit to adjust the reflection coefficient. Based on the received information, it is possible to optimize the trajectory and the passive beamforming to improve the signal reflection for serving the users.

### C. AERIAL IRS IN NOMA NETWORKS

Multiple access techniques have an important role to support massive connectivity for next-generation mobile networks. In order to improve the spectral efficiency and the connectivity of AIRS framework, NOMA techniques can be employed [35]. When these technologies are accurately combined, significant performance enhancements can be achieved, such as more flexibility, efficient resource allocation, and signal coverage area.

In particular, IRS technology introduces a new paradigm in NOMA transmission to opportunistically improve the decoding process. This paradigm increases the flexibility by changing the original order of the users' channel gains. In the uplink of conventional NOMA, where the users are sorted according to their channel conditions, the new paradigm allows that the users to be sorted according to their data requirements, circumventing the problem of strict dependence on the propagation environment and the location of users. Then, reflecting elements of IRS can be dynamically tuned to either maximize or attenuate the rates by each user according to their specific quality of service (QoS). As a result, it is possible to serve a large

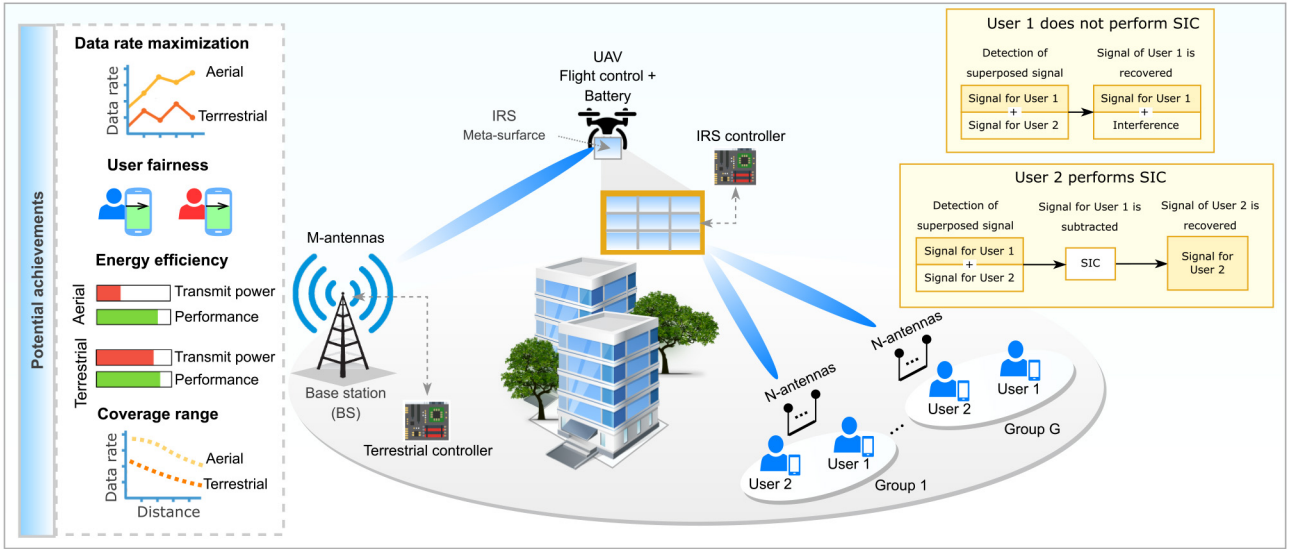


FIGURE 2. Illustration of AIRS in MIMO-NOMA networks (AIRS-NOMA) and potential gains of its integration.

number of users with stringent communication requirements without requiring more energy and time slots. In addition, the performance of conventional NOMA can be enhanced by the supplementary signal diversity generated by the IRS. The integration of IRS in aerial platforms, and the potential gains of its integration in MIMO-NOMA networks are illustrated in Fig. 2.

#### D. AIRS-NOMA NETWORKS: SYSTEM MODEL

Consider a MIMO-NOMA downlink network where one base station ( $S$ ) equipped with  $M$  antennas communicates with multi-antenna users, equipped with  $N$  antennas each, distributed into  $G$  groups with two users ( $D_{gu}$ ) each, where  $g = \{1, \dots, G\}$  and  $u = 1, 2$ , such that  $N \leq M$  and  $G \leq M$  must be satisfied. It is assumed that there is no direct link between the BS and the users due to severe blockage, then an IRS ( $R$ ) with  $K$  reflecting elements is installed at the UAV to enable the communication between the BS and the users. It is considered that the IRS can forward the impinging signals with high directivity so that a signal beam for the  $u$ -th user of the  $g$ -th group does not interfere with another signal beam. The mobile users' devices move randomly and independently in a circular cell, with radius  $r_g$ . The random waypoint model is implemented to simulate the mobility of the users [52], [53]. During all periods of the mobility process, the users randomly choose a new coordinate and move to it at a constant speed. For each time slot of the mobility process, the new location of the users is calculated. In addition, it is assumed that the UAV continuously flies with a constant velocity and variant elevation  $Z$  in a spherical plan of radius  $r_u$ . For a given  $Z$ , the UAV can fly in the following height range:  $Z - r_u \leq z \leq Z + r_u$ , where  $z$  denotes the instantaneous height.

Based on the downlink power-domain NOMA principles [54], the users' message are superimposed at the BS by

SC technique, which consists of superposing the messages of each user by assigning different power coefficients between the users. Then, the BS sends the superimposed signal in the direction of the AIRS. More specifically, the transmitted signal can be written as

$$\mathbf{x} = \sum_{g=1}^G \sum_{u=1}^2 \alpha_{gu} s_{gu} \in \mathbb{C}^{M \times 1}, \quad (1)$$

where  $s_{gu}$  denotes the message of interest of the  $u$ -th user in the  $g$ -th group, and  $\alpha_{gu}$  denotes their respective power allocation coefficient with  $\alpha_{gu} > 0$  and  $\sum_{u=1}^2 \alpha_{gu} \leq 1$ . The channel gain matrices between  $S \rightarrow R_r$  and  $R_r \rightarrow D_{gu}$  can be expressed, respectively, as

$$\mathbf{H}_{SR_r} = \sqrt{\beta_{SR_r}} \mathbf{W}_{SR_r} \in \mathbb{C}^{M \times K}, \quad (2)$$

and

$$\mathbf{H}_{R_r D_{gu}} = \sqrt{\beta_{R_r D_{gu}}} \mathbf{W}_{R_r D_{gu}} \in \mathbb{C}^{K \times N}, \quad (3)$$

where  $\beta_a = \beta_0 d_a^{-\nu}$ ,  $a \in \{SR_r, R_r D_{gu}\}$  denotes the large-scale average channel power gain with  $r = 1, \dots, K$ , in which  $\beta_0$  denotes the average channel power gain at the reference distance  $d_0 = 1$  m,  $d_a$  denotes the distance between  $S \rightarrow R_r$  and  $R_r \rightarrow D_{gu}$ , and  $\nu$  denotes the pathloss exponent.  $\mathbf{W}_a$  denotes the small-scale fading, modeled by the Nakagami- $\mu$  distribution, as in [17]. Without loss of generality, the complex channel gain matrices  $\mathbf{W}_{SR_r}$  and  $\mathbf{W}_{R_r D_{gu}}$  can be expressed as

$$\mathbf{W}_{SR_r} = \begin{bmatrix} |g_{SR_{1,1}}| e^{j\omega_{1,1}} & \dots & |g_{SR_{1,M}}| e^{j\omega_{M,1}} \\ |g_{SR_{2,1}}| e^{j\omega_{1,2}} & \dots & |g_{SR_{2,M}}| e^{j\omega_{M,2}} \\ \vdots & \ddots & \vdots \\ |g_{SR_{K,1}}| e^{j\omega_{1,K}} & \dots & |g_{SR_{K,M}}| e^{j\omega_{M,K}} \end{bmatrix}, \quad (4)$$

and

$$\mathbf{W}_{R_r D_{gu}} = \begin{bmatrix} |g_{R_1 D_{gu},1}| e^{j\omega_{1,1}} & \dots & |g_{R_1 D_{gu},N}| e^{j\omega_{N,1}} \\ |g_{R_2 D_{gu},1}| e^{j\omega_{1,2}} & \dots & |g_{R_2 D_{gu},N}| e^{j\omega_{N,2}} \\ \vdots & \ddots & \vdots \\ |g_{R_K D_{gu},1}| e^{j\omega_{1,K}} & \dots & |g_{R_K D_{gu},N}| e^{j\omega_{N,K}} \end{bmatrix}^H, \quad (5)$$

where  $|g_{a,m}|$  and  $\omega_{m,r} \in [0, 2\pi)$  are, respectively, the magnitude and phase angle between  $m$ -th transmission antenna of the BS and the  $r$ -th reflecting element of the AIRS, with  $m = 1, \dots, M$ .

Since a controller connected to the IRS can smartly adjust the IRS's phase shifts to assist the NOMA transmission, the properties of the AIRS can be characterized via the following diagonal phase-shift matrix

$$\Theta = \text{diag}[\kappa_1 e^{j\theta_1}, \kappa_2 e^{j\theta_2}, \dots, \kappa_K e^{j\theta_K}] \in \mathbb{C}^{K \times K}, \quad (6)$$

where  $\theta_K \in [0, 2\pi)$  denotes the phase-shift occurring at  $r$ -th element of the AIRS, and  $\kappa_K \in [0, 1)$  denotes the fixed amplitude reflection coefficient. In particular, it is very expensive to realize infinite-resolution phase shifters due to hardware limitations. As a result, the complexity to perform the phase-shift increases considerably [37]. In particular, the end-to-end (e2e) channel matrix from the BS to the  $u$ -th user in the  $g$ -th group with aid of the AIRS is given by

$$\tilde{\mathbf{H}}_{gu} = \mathbf{H}_{SR_r} \Theta \mathbf{H}_{R_r D_{gu}} \in \mathbb{C}^{M \times N}. \quad (7)$$

The signal received at the  $u$ -th user in the  $g$ -th group can be expressed as

$$\mathbf{y}_{gu} = \sqrt{P_S} \tilde{\mathbf{H}}_{gu} \mathbf{x} + \mathbf{w}_{D_{gu}}, \quad (8)$$

where  $P_S$  denotes the transmit power of the BS and  $\mathbf{w}_{D_{gu}} \sim \mathcal{CN}(0, \sigma^2)$  denotes the additive Gaussian noise (AWGN).

Analogous to [34], it is considered that the IRS can reflect the signal to a desired point with high directivity and the clusters are separated far enough. Thus, the clusters have a non-overlapping reflection angle and the interference arriving at a specific cluster from other clusters will be extremely small, i.e., it can be neglected. On the other hand, to eliminate the inter-group interference, the signal reception is designed by adopting a zero-forcing receiver. More specifically, the detection matrix can be constructed as follows

$$\hat{\mathbf{H}}_{gu} = [\tilde{\mathbf{H}}_{gu}^H \tilde{\mathbf{H}}_{gu}]^{-1} \tilde{\mathbf{H}}_{gu}^H \in \mathbb{C}^{M \times N}. \quad (9)$$

Given this zero-forcing receiver, the received signal at each user is decoupled from each other. Then, the effective channel power gain between the BS and the  $u$ -th user in the  $g$ -th group with the aid of the AIRS is given by

$$\ddot{\mathbf{H}}_{gu} = \hat{\mathbf{H}}_{gu} (\hat{\mathbf{H}}_{gu})^H \in \mathbb{C}^{M \times M}. \quad (10)$$

Since the symbols will be decoded from the beam that is equivalent to the index  $gg$  of the channel power gain matrix, the highest effective channel gain, the selected beam is denoted as  $\ddot{g}\ddot{g}$ . Then,  $[(\ddot{\mathbf{H}}_{gu})_{\ddot{g}\ddot{g}}]^{-1}$  denotes the effective channel gain observed by the  $u$ -th user in the  $g$ -th group.

Based on available CSI, the users are ordered according to their effective channel gains. Without loss of generality, we assume that the user  $D_{g1}$  has the weakest channel gain, while user  $D_{g2}$  experiences the greatest channel conditions. Then, higher power must be allocated to the user with the worst channel conditions in order to ensure that its data requirements can be achieved, which means that  $\alpha_{g1} > \alpha_{g2}$ . After the user ordering operation, the e2e signal-interference-plus-noise (SINR) for the weakest user in the  $g$ -th group to decode its message is given by

$$\gamma_{g1} = \frac{\tilde{\gamma} \tilde{h}_{g1} \alpha_{g1}}{\tilde{\gamma} \tilde{h}_{g1} \alpha_{g2} + 1}, \quad (11)$$

where  $\tilde{h}_{g1} = [(\ddot{\mathbf{H}}_{g1})_{\ddot{g}\ddot{g}}]^{-1}$  denotes the effective channel gain observed by the weaker user in the  $g$ -th group,  $\tilde{\gamma} = P_S/\sigma^2$  denotes the transmit signal-to-noise ratio (SNR).

Under the assumption of imperfect SIC, the e2e SINR observed by the stronger user in the  $g$ -th group is given by

$$\gamma_{g2} = \frac{\tilde{\gamma} \tilde{h}_{g2} \alpha_{g2}}{\tilde{\gamma} \tilde{h}_{g2} \alpha_{g1} \epsilon + 1}, \quad (12)$$

where  $\tilde{h}_{g2} = [(\ddot{\mathbf{H}}_{g2})_{\ddot{g}\ddot{g}}]^{-1}$  denotes the effective channel gain observed by the strongest user in the  $g$ -th group,  $\epsilon \in [0, 1]$  is the coefficient of imperfect SIC.

The instantaneous achievable rate of the weaker user in the  $g$ -th group can be expressed as

$$R_{g,1} = \log_2(1 + \gamma_{g1}). \quad (13)$$

The e2e instantaneous achievable rate of the stronger user in the  $g$ -th group is given by

$$R_{g,2} = \log_2(1 + \gamma_{g2}). \quad (14)$$

In the next section, we provide in-depth discussions and significant numerical results to support the gains achieved by AIRS in MIMO-NOMA networks.

### III. POTENTIAL ACHIEVEMENTS OF AERIAL IRS-AIDED MIMO-NOMA NETWORKS

In this section, numerical simulations to emphasize the performance gain when AIRS is applied in MIMO-NOMA wireless networks are presented. More specifically, it is discussed and highlighted the performance gain in terms of sum-rate, user fairness, energy efficiency, and coverage range. Performance metrics are evaluated by extensive Monte Carlo simulations that corroborate the advantages of implementing IRS in aerial scenarios.

Taking into account the three-dimensional spatial movement of UAV, we design a downlink AIRS-NOMA network system with  $G$  groups with two mobile users, denoted by user 1 and user 2, respectively. In particular, it is assumed that each node in the network is equipped with multiple antennas and there is no direct link between the BS and the users due to strong fading and physical obstacles. The distance between the BS and the center of the cell of the group 1, group 2, and group 3 is, respectively,

**TABLE 2.** Simulation parameters.

Parameter	Value
Number of users per group ( $U$ )	2
Group cell radius ( $r_g$ )	5 m
UAV height ( $z$ )	$(20 - r_u \leq z \leq 20 + r_u)$ m
Spherical plan radius of UAV ( $r_u$ )	2 m
Number of groups ( $G$ )	3
Number of transmit antennas ( $M$ )	4
Number of receiver antennas ( $N$ )	4
of reflecting elements ( $K$ )	20
Path loss exponent ( $\nu$ )	2.2
PA coefficient for weak user ( $\alpha_{g1}$ )	0.7
PA coefficient for strong user ( $\alpha_{g2}$ )	0.3
Nakagami parameter ( $\mu$ )	2.5
Average channel power gain ( $\beta_0$ )	500
Coefficient of imperfect SIC ( $\epsilon$ )	0, 0.005, 0.01
Distance between BS and AIRS ( $d_{SR}$ )	$(98 \leq d_{SR} \leq 102)$ m
Distance between AIRS and group 1 ( $d_{RD_{1u}}$ )	$(20 - r_g \leq d_{RD_{1u}} \leq 20 + r_g)$ m
Distance between AIRS and group 2 ( $d_{RD_{2u}}$ )	$(50 - r_g \leq d_{RD_{2u}} \leq 50 + r_g)$ m
Distance between AIRS and group 3 ( $d_{RD_{3u}}$ )	$(100 - r_g \leq d_{RD_{3u}} \leq 100 + r_g)$ m

100 m, 150 m, and 200 m. When TIRS is deployed, it is assumed that the TIRS is positioned at 80 m from the BS. The users of each group are randomly distributed in a cell of radius  $r_g = 5$  m, and classified according to their channel conditions. Without loss of generality, centralized design is employed in our simulations. Unless otherwise specified, the simulation parameters follow the Table 2.

It is noteworthy that no optimization method is used to configure the reflecting elements in this paper. Then, the phase shift is randomly and uniformly generated in  $[0, 2\pi)$ . From a deployment perspective, we assume that the network control structure follows the centralized deployment, where the AIRS is controlled by a terrestrial central controller installed at the BS. By using centralized deployment, all processing tasks are employed by the BS, such as estimation protocols. In addition, we consider that the terrestrial controller is able to estimate the CSI of all propagation links. As a benchmark performance, we compare our results with TIRS-NOMA presented in [34] without considering massive MIMO and direct link between the BS and users, and with conventional relaying ADF-NOMA method.

### A. DATA RATE MAXIMIZATION

To demonstrate the potential of AIRS-NOMA, we first discuss the performance gains in terms of sum-rate for each user group. Then, we compare the obtained results with TIRS-NOMA and ADF-NOMA. According to the NOMA principles, the BS sorts the users based on their respective channel conditions so that more power can be allocated to the user with the worst channel conditions. Without loss of generality, it is assumed that user 1 has unfavorable channel conditions and requires a low data rate. On the other hand, user 2 has better channel conditions and requires a high data rate. At the BS, the signals of the two users are superimposed with different power levels by the SC technique and transmitted to the AIRS, which passively reflects signals from

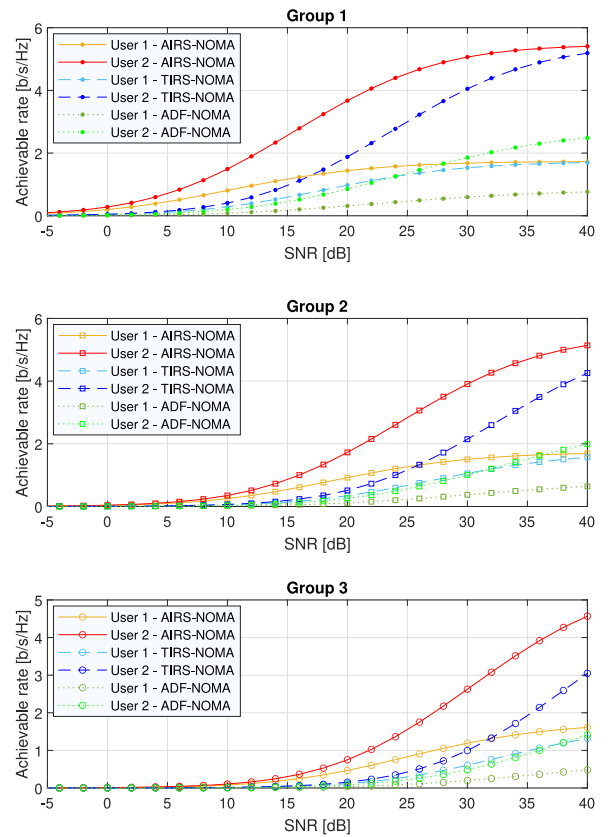


**FIGURE 3.** Achievable rate versus the transmit SNR for each user group. ( $K = 20$ ,  $\alpha_{g1} = 0.7$ ,  $\alpha_{g2} = 0.3$ , and  $\epsilon = 0.01$ ).

BS to users. In the receiver, the users can employ SIC to decode the transmitted messages.

Fig. 3 presents the achievable rate versus the transmit SNR for both weak and strong user for each group of users. For comparison, TIRS and ADF deployment are applied. One can observe that for all groups the AIRS outperforms the TIRS deployment. This performance is related to the



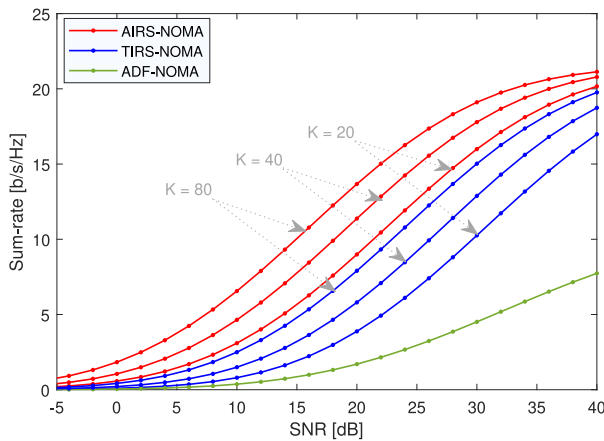


FIGURE 4. Sum-rate versus transmit SNR for different number of reflecting elements. ( $\alpha_{g1} = 0.7, \alpha_{g2} = 0.3$ , and  $\epsilon = 0.01$ ).

coverage holes and blind spots that can occur during the transmission process, and virtual LoS links might not be formed even with the aid of the IRS. On the other hand, the UAV placement can be adjusted to maintain LoS links. Once the favorable UAV placement is found, one can adjust the IRS reflection parameters to reflect the signal in the desired direction. On the other way, the UAV can remain static to minimize energy consumption until it is necessary to adjust its position again to ensure the LoS component. However, one can also see that the greater is the distance between AIRS and a group of users, the worse is the rate achieved by this group. This reinforces the need to improve propagation in far-field scenarios. In particular, the integration of IRS in the aerial platform can provide more flexibility to assist terrestrial users. In addition, the performance achieved by using ADF as relaying protocol is evidently low when compared to both AIRS and TIRS schemes.

In addition, Fig. 4 illustrates the average sum-rates versus SNR for deployment with AIRS-NOMA, TIRS-NOMA, and without IRS for a different number of reflecting elements of the IRS ( $K$ ). One can observe that the performance of the sum-rate enhances as the number of reflecting elements increase. In particular, higher reflecting array gain can be explored to maximize the effective channel gain and improve the reliability of the received signal. When IRS is installed at the UAV, one can achieve better service quality to the overall network due to the capability to maintain the LoS links even in an environment with a high probability of link obstruction. As a result, significant benefits in sum-rate gain can be achieved. For example, when the SNR is 20 dB, the TIRS-NOMA with  $K = 80$  achieves a performance of 7.9 bits/s/Hz, while AIRS-NOMA with  $K = 80$  can reach 13.6 bits/s/Hz, that represents a performance gain of approximately 5.7 bits/s/Hz. We also observe that when IRS is employed, the performance gain is more pronounced than conventional ADF-NOMA for all SNR values. These results indicate that AIRS-NOMA transmission is a promising framework.

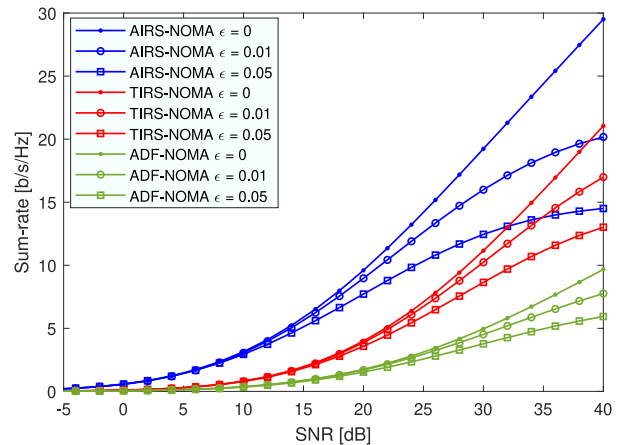


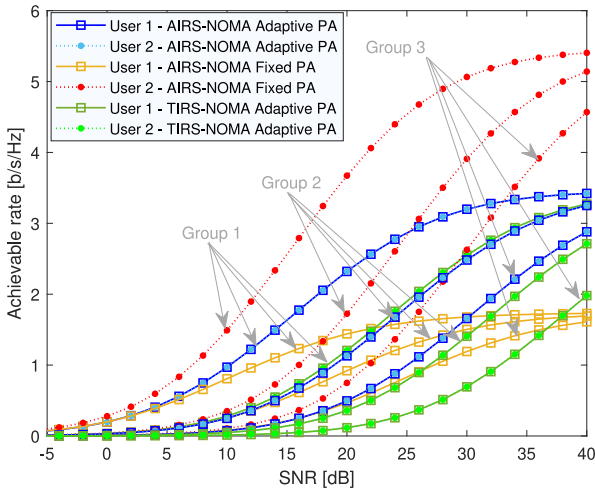
FIGURE 5. Sum-rate versus transmit SNR for different coefficients of imperfect SIC ( $\epsilon$ ). ( $K = 20, \alpha_{g1} = 0.7, \alpha_{g2} = 0.3$ ).

Fig. 5 presents the impact of imperfect SIC factor through the sum-rate of the system. As a performance comparison, we vary  $\epsilon$  and compare the performance between AIRS-NOMA, TIRS-NOMA, and ADF-NOMA schemes. One can see that the errors due to imperfect SIC can cause severe damage to the system. On the other hand, as expected, when  $\epsilon = 0$  is employed the performance in terms of sum-rate is expressively better. For example, when the SNR is 30 dB, the AIRS-NOMA scheme achieve a sum-rate of 19.23 b/s/Hz for  $\epsilon = 0$ , but with  $\epsilon = 0.05$  the sum-rate obtained is 12.44 b/s/Hz, which represents approximately a loss of 6.78 b/s/Hz.

## B. USER FAIRNESS

Since the NOMA technique is used as the transmission scheme, the spectrum's usage efficiency can be improved by superimposing the users' signals, exploring the same resource block. By assuming that the users subscribe to the same traffic service that requires a minimum data rate to be acceptably provided, one can guarantee that all users are served equally throughout the communication process by the efficient power allocation (PA) method. By dynamically allocating power coefficients, it is possible to provide a portion of power for the user with a better conditions channel, called user 2, which performs the SIC correctly. Meanwhile, the remaining power is applied to maximize the weak user's rate, called user 1. More details about the dynamic power allocation strategy can be found in [3].

Fig. 6 depicts the achievable rate for each user at the  $g$ -th group versus transmit SNR for different PA methods. For comparison purposes, we employ both fixed and the adaptive PA policy [3]. It is interesting to observe from Fig. 6 that the adaptive PA can significantly improve the rate performance of the user with the worst channel conditions. However, the main disadvantage of this approach is that the performance of the user with better channel conditions is degraded. Since the main idea of this strategy is performing a balance between users' rates, the strong user can be penalized in order to guarantee that the weak user could reach the



**FIGURE 6.** Achievable rate versus transmit SNR for AIRS-NOMA system and TIRS-NOMA system with adaptive PA and fixed PA. When the fixed PA scheme is applied, it is assumed that the power allocation coefficients applied to the users 1 and 2 of the  $g$ -th group are, respectively, ( $K = 20, \alpha_{g1} = 0.7, \alpha_{g2} = 0.3$ , and  $\epsilon = 0.01$ ).

same service traffic. On the other hand, one can observe that by the adequate deployment of IRS, it is possible to significantly improve the network performance. By exploring the UAV features, AIRS achieves better performance than terrestrial deployment. Compared with the rate performance of groups 1 and 2, group 3 presents a lower performance due to the distance in relation to AIRS, but the result obtained is expressively superior to the result obtained by TIRS-NOMA. This result indicates that AIRS-NOMA systems can provide user fairness while bringing high-performance to the system in comparison with terrestrial framework.

In Fig. 7, it is investigated the relation between resource allocation fairness in terms of transmit SNR. The Jain's fairness index, given by  $J_g = (R_{g,1} + R_{g,2})^2 / [2((R_{g,1})^2 + (R_{g,2})^2)]$ , is used as a fairness metric. As a performance benchmark, the conventional fixed PA policy has been adopted. One can see that the adaptive PA can provide optimal user fairness for all SNR values, ensuring that all network users are served equally throughout the communication process. If all users get the same rate amount, then the fairness index is 1 and the system is totally fair. On the other hand, for fixed PA, there is a disparity between rates and, consequently, the fairness index decreases. The adaptive strategy favors all the users of the system, ensuring fair rate resources independently of channel conditions.

### C. ENERGY EFFICIENCY

In the literature, it has been proved that the NOMA technique can significantly increase the spectrum and energy efficiency of the communication networks due to the capability to allow multiple users to share the same resources. In parallel, studies in the field of IRS prove that this promissory technology can improve the data rates of users without requiring more transmit power, but only smartly adjusting the reflecting elements to increase the channel gains. Since a centralized IRS

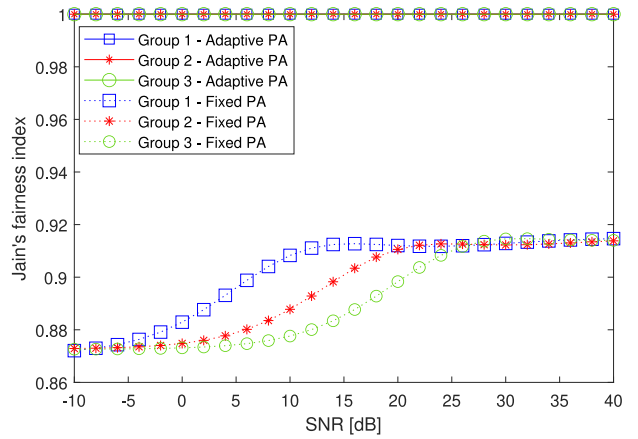


**FIGURE 7.** Jain's fairness index versus SNR for different adaptive PA schemes. When the fixed PA scheme is applied, it is assumed that the power allocation coefficients assigned to the users 1 and 2 of the  $g$ -th group are, respectively, ( $K = 20, \alpha_{g1} = 0.7, \alpha_{g2} = 0.3$ , and  $\epsilon = 0.05$ ).

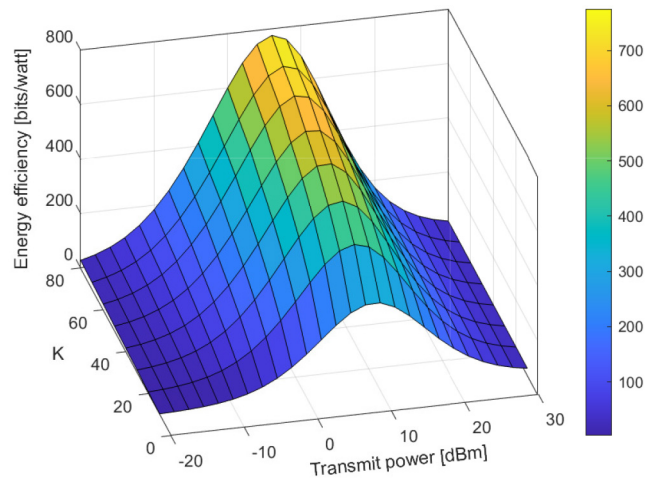


**FIGURE 8.** Energy efficiency of the system versus the number of reflecting elements of the IRS and the transmit power for AIRS-NOMA systems. ( $\alpha_{g1} = 0.7, \alpha_{g2} = 0.3$ , and  $\epsilon = 0.01$ ).

deployment is considered, the energy required by IRS is only directed for the reconfigurability of reflecting elements, which can be employed by low-power electronics. However, considering the hardware constraints, it is not always feasible to deploy a centralized IRS when the number of reflecting elements is large. To achieve a trade-off between the number of reflecting elements and energy consumption, the features of IRS can be integrated into the UAV in order to strengthen the received signal at the ground users due to the high operating altitude of the UAV which increases the coverage area through efficient dynamic 3D beamforming.

A practical demonstration of the integration of the IRS into aerial platforms for performance gains in terms of energy efficiency, can be seen in Fig. 8, which is defined as  $B \cdot \bar{R}_{gu} / P_{total}$ , where  $B$  denotes the bandwidth,  $\bar{R}_{gu}$  denotes the system's sum rate, and  $P_{total}$  denotes the transmit power [55]. In particular, the energy efficiency performance for different number of reflecting elements and transmit power levels.

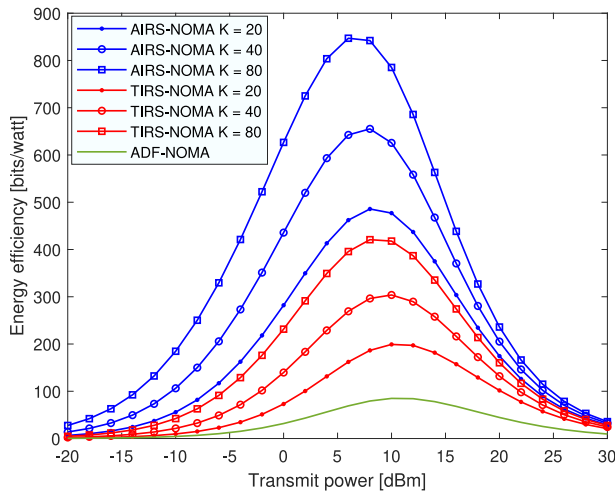


FIGURE 9. Energy efficiency versus transmit power for different number of reflecting elements. ( $\epsilon = 0.01$ ).

One can observe that the greater the number of reflecting elements, the higher the energy efficiency that the AIRS-NOMA system is able to achieve. It is noteworthy that the energy neutrality in the elements of the IRS is assumed. In addition, one can see that there exists a trade-off between the number of reflecting elements,  $K$ , and transmit power levels to maximizes energy efficiency.

Based on the previous result, we investigate the performance of AIRS-NOMA for different number of reflecting elements and different framework scenarios. Specifically, Fig. 9 presents the energy efficiency curves versus transmit power for different number of reflecting elements and TIRS-NOMA and ADF-NOMA counterpart schemes. One can observe that the AIRS-NOMA systems have the ability to achieve enhanced energy efficiency compared to terrestrial and conventional deployment. By exploring aerial mobility, we can achieve higher performance gains with less transmit power. One can see the significant gain in performance when  $K$  increases due to the passive energy-consumption nature. In this way, the signal beam can be improved without need of excessive energy cost. For example, when the transmit power is 10 dBm, the AIRS-NOMA with  $K = 20$  reaches a performance of 477 bits/watt, while with  $K = 80$ , the energy-efficiency achieves a performance of 785 bits/watt, that represent a gain performance of 308 bits/watt. In particular, to contribute with this good performance, there is an energy consumption compensation between the IRS and UAV. The UAV does not need to be in constant movement, as the IRS can form virtual LoS Links. On the other hand, when the IRS cannot guarantee this link due to the dynamic nature of ultra-dense environments, the UAV can dynamically change position to guarantee the LoS link. Then, the UAV can remain static until further intervention is required.

In order to show how energy-efficient AIRS can become in scenarios where the IRS is not neutral and with perfect and imperfect SIC, Fig. 10 presents the energy efficiency curves

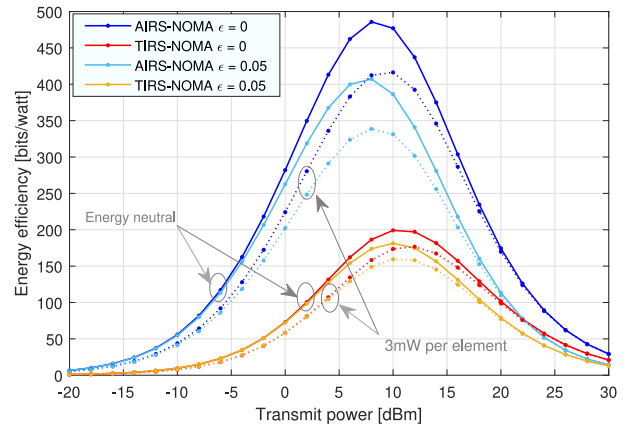
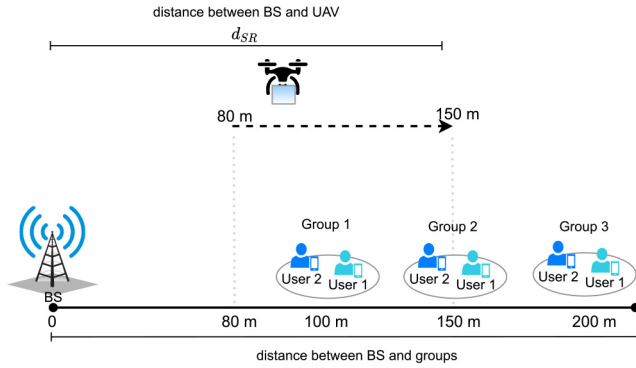


FIGURE 10. Energy efficiency versus transmit power for AIRS-NOMA and TIRS-NOMA systems. Non-neutral power consumption and imperfect SIC are considered. ( $K = 20, \alpha_{g1} = 0.7$  and  $\alpha_{g2} = 0.3$ ).

for energy neutral and energy non-neutral scheme with perfect and imperfect SIC. One can observe the impact caused by the imperfect SIC. For example, when the transmit power is 10 dBm and the neutral power consumption is considered, the AIRS-NOMA with  $\epsilon = 0.05$  can reach a performance of 386.3, bits/watt, while with  $\epsilon = 0$ , the energy efficiency increase up to 477 bits/watt, that represent a performance gain of approximately 90.68 bits/watt. In addition, we compare the obtained results with TIRS-NOMA framework. Due to the non-neutral power consumption of the circuit, one can see that the energy efficiency decrease. However, the performance obtained by AIRS-NOMA scheme is significantly superior to obtained using TIRS-NOMA scheme. It is noteworthy that if the energy neutrality assumption can be satisfied, the energy efficiency will significantly be increased as the number of reflecting elements increase.

#### D. COVERAGE RANGE

It was discussed that the IRS can form virtual LoS links by adjusting the reflecting elements but, when these links cannot be formed due to obstructions, the UAV can be repositioned to help establish high data rates and reliable transmissions. As a result, users' service requirements can be met, leading to good network performance. In particular, Fig. 11 illustrates the scenario used to analyze the performance in terms of coverage range. To investigate the impact of AIRS-NOMA scheme, Fig. 12 presents the sum-rate versus distance for different IRS deployments and the conventional ADF-NOMA relaying protocol. We set the transmit SNR to  $\rho = 30$  dB and assume that the distance between the BS and AIRS is  $d_{SR}$ , and the distance between the BS and the center of the cell of the group 1, group 2, and group 3 are, respectively, 100 m, 150 m and 200m. One can observe that the performance of AIRS-NOMA decreases when the distance between the users increases. In contrast to the TIRS-NOMA scheme, the AIRS-NOMA scheme has more potential to establish strong LoS links with the users due to the relatively higher altitude of UAV, thus reducing the coverage



**FIGURE 11.** Centralized design: Illustration of the scenario used to simulate the results in Figure 12.

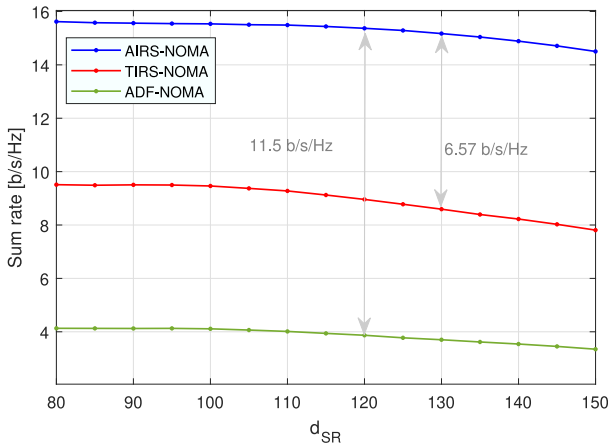


**FIGURE 12.** Sum-rate versus distance for AIRS-NOMA, TIRS-NOMA, and ADF-NOMA deployments. ( $\bar{\gamma} = 30$  dB,  $K = 20$ , and  $\epsilon = 0.01$ ).

holes or blind spots with them. For example, when the distance between the BS and the AIRS is 130 m, the TIRS-NOMA scheme can reach a sum-rate of 8.59 b/s/Hz, while with the AIRS-NOMA system, the sum-rate increases up to 15.17 b/s/Hz, which represents a gain of 6.57 b/s/Hz. In addition, when  $d_{SR} = 120$  m the AIRS-NOMA outperforms conventional ADF-NOMA with a performance gain of approximately 11.5 b/s/Hz. This result clearly demonstrates that, by exploiting the AIRS capabilities, the MIMO-NOMA scheme can effectively extend the coverage area.

To summarise the main difference between AIRS-NOMA, TIRS-NOMA, and ADF-NOMA, Table 3 presents an overview of the advantages and disadvantages of each framework.

#### IV. RELEVANT CHALLENGES AND RESEARCH OPPORTUNITIES

In this section, we provide potential challenges and promising research possibilities to effectively deploy AIRS-NOMA networks.

##### A. CHANNEL MODEL AND ESTIMATION STRATEGIES

In a general AIRS-NOMA network, the e2e channel (i.e., the channel from terrestrial BS to the ground users through

**TABLE 3.** Comparison of AIRS-NOMA with other frameworks.

Framework	Advantage	Drawback
AIRS-NOMA	Rate maximization User fairness High energy efficiency Coverage range Low hardware cost	High sensitive to channel Uncertainly due to the fast mobility Battery UAV
TIRS-NOMA	User Fairness Low hardware cost	Limited coverage range Difficult to estimate CSI
ADF relay	Decodes the signal and forwards a regenerated copy	High energy consumption Low data rate

each element of AIRS) is composed of three components. More specifically, the channel responses between the terrestrial BS and AIRS, the AIRS's reflection matrix, and the channel responses between AIRS and ground users link. The combination of these three components, BS-AIRS-user, can be represented by a multiplicative channel model, where each element of AIRS's reflection matrix receives the signal from the BS, and then, via a smart controller that enables dynamic adjustment of amplitude and phase shift, reflects the impinging signal. Since IRS is coupled to the UAV, the system experiences a rapid dynamic mobility pattern. This mobile operation requires real-time channel estimation and reconfiguration, taking into account fading and shadowing effects. Furthermore, the smart controller also plays the role of dynamic exchanging information between the AIRS and terrestrial BS. Based on this, one can ask how is it possible to enable real-time reconfigurability under mobile conditions using as low a processing effort as possible due to the hardware limitation of the IRS.

Channel design and estimation for AIRS-NOMA are critical research topics due to its dynamic CSI-dependence to configure the reflecting elements, the passive nature of AIRS elements, and the multi-user nature of NOMA. To develop robust aerial channel models, one needs to take into account factors that could affect the system performance, such as IRS reflection coefficients, elements' mutual coupling, reflection loss, fluctuations and misaligned signal beams due to the UAV mobility, and NOMA decoding order, since the decoding order is not determined by channel conditions. Unlike the conventional technologies, the passive IRS architecture is not composed of a transceiver chain but is equipped with meta-materials to reflect the signal in the desired direction. Then, the IRS structure cannot employ complex signal processing tasks. In addition, the most conventional communication system operates in far-field conditions, i.e., the distance between the users and the transmitter/receiver antennas is supposed to be large. On the other hand, in an AIRS-NOMA network, one cannot guarantee that the distance between users and its serving IRS is far enough to operate only as a far-field regime or small enough to operate as a near-field regime due to the UAV mobility. Thus, the system must be dynamically adapted to decide which regime it should operate.

Another important factor that should be strictly considered in the channel modeling is the size of the AIRS. In particular, channel coefficients are proportional to the number of reflecting elements, which induces the cascaded channel estimation problem. To circumvent this issue when the number of AIRS reflecting elements is not large, a decomposition method for cascaded channel estimation can be employed for each AIRS element to transform the cascaded channel into a series of sub-channels by each user [56], [57]. However, when the number of AIRS reflecting elements and the number of users increase, this method is difficult to implement due to the high signaling overhead. Unlike the fixed semi-passive IRS deployment, where it is possible to estimate the global CSI by integration of at least low-power sensors to reconfigure each AIRS's element [7], AIRS under mobility imposes extra estimation difficulty due to the need to realize fast real-time IRS configuration, which leads to high computation complexity for the time-varying channels. In consequence, additional sensing components are required to employ sophisticated channel estimation protocols, which can potentially lead to high-energy consumption. From an implementation perspective, current channel estimation methods are not appropriate to explore the benefits of the AIRS-NOMA networks. One approach to circumvent this problem consists into insert additional sensing components at the terrestrial BS to control and optimize channel estimation methods. If these methods are employed by terrestrial control, the BS can provide high computational power to estimate the channel and the processing cost at the IRS might be minimized. However, due to the fast time-varying wireless environment and dynamic QoS requirements of the users, the AIRS control layer must send data of the environment and send measurements to the ground controller for optimization of channel estimation protocols. Then, the AIRS control layer needs additional sensing components with receiver chains to enable information exchange with BS. Therefore, efficient algorithms should be carefully developed to maintain the low complexity as possible and to avoid operations that require high-energy consumption.

**B. DEPLOYMENT STRATEGY**

As previously introduced, the complexity of the channel acquisition increase as the number of users and reflecting elements of IRS increase. In addition, from a NOMA implementation perspective, there is a limited number of users that can be served in the same resource block. However, the design of efficient user clustering schemes plays an important role to exploit the benefits of AIRS-NOMA networks to support the massive number of devices [33]. But, to jointly enhance the coverage area, the proposition of deployment strategies to efficiently explore the AIRS-NOMA framework arises as one important research topic. By designing a practical deployment of AIRS-NOMA network under real-time reconfigurability, especially under mobility conditions that demand dynamic IRS configuration, it is needed to take

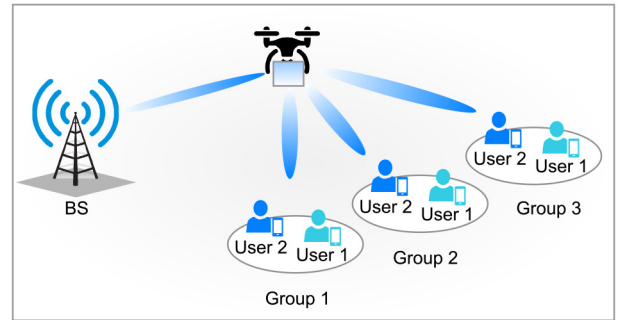


FIGURE 13. Centralized deployment.

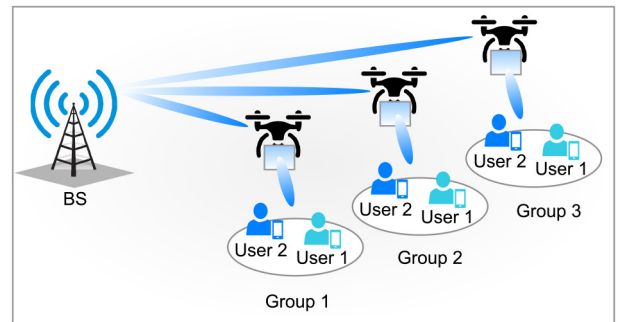
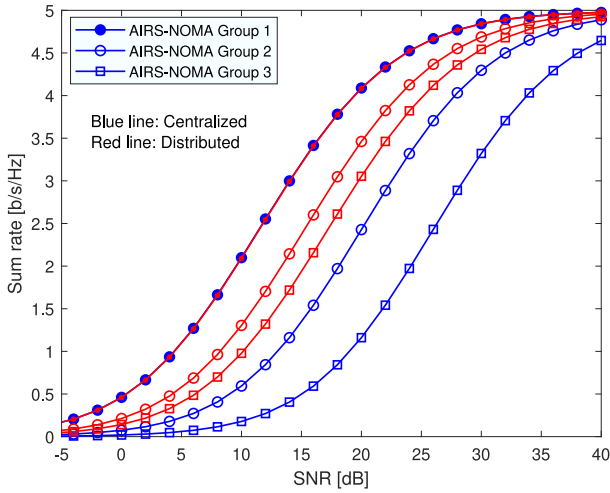


FIGURE 14. Distributed deployment.

into account the heterogeneous QoS requirements and the heterogeneous mobility profiles.

To circumvent these issues, cluster-based strategies are approaches that aim to serve multiple users according to your requirements with a passive 3D beam. In particular, the users can be clustered in centralized and distributed designs. In the previous results, we employed a centralized design where the users are partitioned into multiple clusters and each group is served from passive beamforming of a single centrally deployed AIRS, as illustrated in Fig. 13. This strategy is ideal for cases where groups of users are not separated by large distances, where the AIRS forms multiple independent beams to each users' group so that their channel gains could be dynamic enhanced, offering additional degrees-of-freedom in the time, frequency, and spatial domains. Despite the above advantages, a large number of reflecting elements is required to improve the 3D beamforming of each group. In consequence, the complexity and energy consumption increase, since the energy neutrality assumption cannot be satisfied and the structure must be equipped with low-power electronics to enable the IRS's reconfigurability capability. In addition, due to the proximity, the signals reflected by one AIRS to a specific cluster might be a strong impact on the reception performance of other clusters. On the other hand, the distributed design can be employed to circumvent cluster interference. In this distributed strategy, each cluster is served by distinct beamforming AIRS, as illustrated in Fig. 14. As a result, the signals reflected by one IRS for a specific cluster have a low impact on the performance of the



**FIGURE 15.** Sum-rate versus SNR for AIRS-NOMA system with centralized and distributed deployment. For centralized deployment, the approximate distance between the AIRS and the group 1, group 2, and group 3 are, respectively, 20m, 50m, 100m. For distributed deployment, the approximate distance between the AIRS and a specific group is 20 m. ( $K = 20, \epsilon = 0.01, \alpha_{g1} = 0.7$ , and  $\alpha_{g2} = 0.3$ ).

other clusters due to the relatively large distances. However, this strategy is not always feasible to deploy due to the demand for an excessive amount of energy to support the hardware. Since both described strategies offer advantages and disadvantages, it is needed to identify scenarios feasible to deploy each strategy such that satisfy all the requirements of NOMA transmission. From the implementation perspective, a more flexible design will be a hybrid IRS deployment to achieve a trade-off between them.

Fig. 15 illustrates the performance in terms of sum-rate for both centralized and distributed design. These results demonstrate the good performance when AIRS is designed in near-field conditions to the users, i.e., when an AIRS is located nearly of a specific user group. On the other hand, a distributed mode requires higher deployment cost. Thus, the implementation scenario must be carefully studied to ensure the efficient deployment of AIRS. In addition, a new research perspective arises to employ efficiently AIRS in far-field conditions in order to verify its viability.

### C. TERAHERTZ (THZ) COMMUNICATIONS

Research efforts have been made along the last years on the IRS-enhanced THz communications field. However, most of these efforts are related to terrestrial IRS-enhanced THz communications [58], [59]. In contrast with communications based on microwave and millimeter waves, THz communication achieves ultra-high transmission rates from hundreds of gigabits per second with frequency bands extremely narrow [60]. This feature results in the formation of a signal beam much narrow, which can produce high attenuation and, consequently, brings out performance damage. In particular, it is hard to perform the control of these beams. To tackle this challenge, IRS can be used to design the signal beam due to

the ability to smartly manipulate and design the impinging waves.

As presented in the previous section, AIRS-NOMA framework can provide enormous performance gains to the system in terms of data rate, coverage range, and energy efficiency when compared with TIRS-NOMA scheme. By considering aerial scenarios, some works have been exploring the integration of AIRS-empowered THz communication [61], [62]. Despite the benefits achieved by the integration of AIRS-NOMA and THz communication, there is a high attenuation THz channel that will introduce new challenges to the AIRS-NOMA communication. Specifically, channel measurements and modeling of THz waves at the sufficiently realistic mobility model must be adequate to the propagation peculiarities of AIRS-NOMA, such as path-loss models, both far-field and near-field transmission, practical phase-shift model, and beamforming control.

In addition, the decoding complexity of NOMA systems is another important challenge to be investigated when THz communication is considered. Although the THz band can support many connected devices, the decoding complexity for NOMA communication to support the devices can increase substantially. Interestingly, the IRS is one of the most promising solutions due to the capability to tune the channel conditions of the user by smartly adjusting the reflecting elements [34]. By considering AIRS, it is possible to improve spectrum efficiency and get good coverage capacity to allow more users to connect to the network even at a high distance from BS. In addition, due to the strong directivity of THz waves, the LoS THz waves can be easily blocked by obstacles. Thus, the AIRS framework plays an important role in THz communication due to the ability to improve the LoS path. As far as we know, there are no works that integrate AIRS-NOMA in THz communications. Based on the guidance provided, there are emerging challenges and significant problems that will be faced in future research in AIRS-NOMA empowered THz communication.

### D. REINFORCEMENT LEARNING IN AIRS-NOMA NETWORKS

To overcome the highly dynamic environment and, effectively, to exploit the benefits of integrating IRSs in the UAV-aided NOMA systems, machine learning techniques applied in communication systems have been arisen as a powerful solution due to the learning features. In particular, RL methods are a branch of machine learning whose main characteristic is the learning of the ideal strategy by exploring unknown environments based on real-time data. More specifically, RL consists of an interactive algorithm that provides one representation of the particulars in an environment by taking actions and receiving rewards. A typical RL-based model for an AIRS-NOMA network is designed to take into consideration four components: agents (BS/UAV/IRS), states (interactions in real-time with the environment), actions (decision-making according to the current

state), and rewards (since the action is carried out, the agent obtains a reward or penalty) [8].

The RL-based solutions have the advantage of requiring low training overhead, which makes them practical in a real-time reconfiguration of the IRS. Based on this, the design and deployment of an AIRS-NOMA network can be powerfully optimized by RL methods. In addition, flexible NOMA decoding order design can be proposed by efficient power allocation policy in an effort to maximize the sum-rate and to guarantee successful SIC while opportunistically exploring the time-varying data requirement of users. To circumvent the cascaded channel estimation problem, RL algorithms can be designed to reduce the overhead of CSI acquisition by learning both from the environment and from the feedback of the users, resulting in a fast adaption to the dynamic environment and directly optimizing both the beamformers at the BS and the reflecting elements at the IRS. From the point of view of security, RL methods can be used to learn the external and internal eavesdropping features on a network. Considering that the CSI of the eavesdropper is a challenge to acquire in practice, the proposition of RL methods can facilitate the identification of potential eavesdroppers, and effectively prevent information leakage and improve the legitimate reception quality scenarios.

Since RL methods allow agents to improve their capabilities based on the real-time experience of the environment, models can be formulated to smartly control and optimize the network to generate a trade-off between network capacity and energy consumption. In particular, the UAVs are powered by onboard batteries that usually have limited capacity and lifetime. Then, energy harvesting technologies [63], such as wireless power transfer [64], can be used to mitigate the impact of limited energy and battery lifetimes. These technologies can be empowered by RL-based algorithms to achieve efficiently a trade-off between the high energy demand of the UAV and the limited battery capacities, even under scenarios with high mobility. For example, transmit power and energy consumption of UAV can be improved by optimizing the trajectory of UAV, practical beamforming models for AIRS and BS can be designed by efficiently phase shift.

#### E. AIRS STANDARDIZATION

In the standardization context, research efforts are carried out in the field of IRSs. Due to the potential that IRS technology provides, many universities and research institutions have gradually increased their investments in IRS research. In particular, there are two possible paths for IRS standardization in 3rd Generation Partnership Project (3GPP). First, study items will be performed on one or multiple practical scenarios and channel models in Release 18, and then the work item process will be started in Release 19. Another possible path may be to standardize IRS as part of 6G standards, along with other new features for 6G. This is possible because of can be harmoniously combined with other expected technologies for beyond 5G (B5G) systems.

In June 2021, a new industry specification group (ISG) on IRS was approved by the European Telecommunications Standards Institute (ETSI) [65]. Specifically, three new work items were approved, which consist of channel modeling, use cases, deployment scenarios, and impact to current standards. In [66], the authors provide an industrial viewpoint and a roadmap in order to make IRSs industrially feasible. The authors discussed the relevance of the IRS technology in the latest wireless communication standards, the challenges to commercialize IRSs, and highlight the current and future standardization activities for the IRS technology.

On the other hand, in the aerial context, there has already been much activity in the work groups of 3GPP to ensure that the 5G and B5G system will meet the connectivity needs of Unmanned Aerial Systems (UAS). Specifically, Release 17 - 5G Enhancement for UAVs (TS22.125; TS22.261) [67], is not complete and 3GPP has been making efforts to complete it with a focus on B5G systems and already thinking about possible improvements in Release 18. Based on this, substantial investment from research and businesses is expected in the next years to reach fast progress in the field of implementing, testing, and realistic prototypes in the context of AIRS.

#### V. CONCLUSION

In this article, the integration of AIRS with MIMO-NOMA technique was investigated. We provided a comprehensive discussion of the AIRS-NOMA network and performance comparison between aerial and terrestrial deployment, including fundamentals, potential achievements of efficient integration, and future challenges. Numerical simulations were presented to demonstrate that AIRS-NOMA scheme can be considered as a key enabler of future wireless communication. The obtained results supported our insightful discussions by comparing AIRS-NOMA with achieved results by TIRS-NOMA, and ADF-NOMA deployment, in which the robustness of AIRS-NOMA was confirmed. Specifically, the integration has the capability to extend the communications coverage, increase the sum-rate, enhance user fairness, and improve energy efficiency due to the capacity of enabling long-range communication, providing dynamic and adaptive coverage range to serve the users by compensating the power consumption of UAV and IRS during the communication process. In addition, challenges to inspire future research about the integration of AIRS-NOMA were highlighted. In particular, we discussed channel modeling and estimation challenges associated to real-time reconfigurability of AIRS under mobility conditions and discussed the deployment design based on cluster-based strategies for AIRS-NOMA network, such as centralized and distributed strategies. In general, when AIRS is designed as distributed strategies with near-field conditions for each user group, the performance in terms of data rate is better, but deployment cost is higher. On the other hand, centralized deployment presents simplified maintenance, reduced deployment cost, and a data rate higher than terrestrial

deployment. These features make centralized deployment viable in suburban and rural areas, and in environmental disaster scenarios. In addition, we also discussed the integration of AIRS-NOMA with THz communication, and potential solutions based on RL methods to decrease the overhead of the CSI acquisition and improve the energy consumption performance of the network.

## REFERENCES

- [1] Cisco. "Global mobile data traffic forecast update, pp. 2017–2022." Feb. 2019. [Online]. Available: <https://www.statista.com/statistics/271405/global-mobile-data-traffic-forecast/>
- [2] Y. Yuan *et al.*, "NOMA for next-generation massive IoT: Performance potential and technology directions," *IEEE Commun. Mag.*, vol. 59, no. 7, pp. 115–121, Jul. 2021.
- [3] B. K. S. Lima, D. B. da Costa, L. Yang, F. R. M. Lima, R. Oliveira, and U. S. Dias, "Adaptive power factor allocation for cooperative full-duplex NOMA systems with imperfect SIC and rate fairness," *IEEE Trans. Veh. Technol.*, vol. 69, no. 11, pp. 14061–14066, Nov. 2020.
- [4] M. Mozaffari, W. Saad, M. Bennis, Y.-H. Nam, and M. Debbah, "A tutorial on UAVs for wireless networks: Applications, challenges, and open problems," *IEEE Commun. Surveys Tuts.*, vol. 21, no. 3, pp. 2334–2360, 3rd Quart., 2019.
- [5] X. Yuan, Y.-J. A. Zhang, Y. Shi, W. Yan, and H. Liu, "Reconfigurable-intelligent-surface empowered wireless communications: Challenges and opportunities," *IEEE Wireless Commun.*, vol. 28, no. 2, pp. 136–143, Apr. 2021.
- [6] Q. Wu and R. Zhang, "Towards smart and reconfigurable environment: Intelligent reflecting surface aided wireless network," *IEEE Commun. Mag.*, vol. 58, no. 1, pp. 106–112, Jan. 2020.
- [7] M. Di Renzo *et al.*, "Smart radio environments empowered by reconfigurable intelligent surfaces: How it works, state of research, and road ahead," *IEEE J. Sel. Areas Commun.*, vol. 38, no. 11, pp. 2450–2525, Sep. 2020.
- [8] Y. Liu *et al.*, "Reconfigurable intelligent surfaces: Principles and opportunities," *IEEE Commun. Surveys Tuts.*, vol. 23, no. 3, pp. 1546–1577, 3rd Quart., 2020.
- [9] M. Munochiveyi, A. C. Pogaku, D.-T. Do, A.-T. Le, M. Voznak, and N. D. Nguyen, "Reconfigurable intelligent surface aided multi-user communications: State-of-the-art techniques and open issues," *IEEE Access*, vol. 9, pp. 118584–118605, 2021.
- [10] Y. Jia, Q. Jingping, K. Abila, and A. Mohamed-Slim. "Non-terrestrial communications assisted by reconfigurable intelligent surfaces." Sep. 2021. [Online]. Available: <https://arxiv.org/abs/2109.00876>
- [11] X. Pang *et al.*, "When UAV meets IRS: Expanding air-ground networks via passive reflection," *IEEE Wireless Commun.*, vol. 28, no. 5, pp. 164–170, Oct. 2021.
- [12] S. Alfattani, W. Jaafar, Y. Hmamouche, A. Yongacoglu, N. Dao, and P. Zhu, "Aerial platforms with reconfigurable smart surfaces for 5G and beyond," *IEEE Commun. Mag.*, vol. 59, no. 1, pp. 96–102, Jan. 2021.
- [13] H. Lu, Y. Zeng, S. Jin, and R. Zhang, "Enabling panoramic full-angle reflection via aerial intelligent reflecting surface," in *Proc. IEEE Int. Conf. Commun. Workshops (ICC Workshops)*, Jul. 2020, pp. 1–6.
- [14] L. Haiquan, Z. Yong, J. Shi, and Z. Rui. "Aerial intelligent reflecting surface: Joint placement and passive beamforming design with 3D beam flattening." Nov. 2020. [Online]. Available: <https://arxiv.org/abs/2007.13295>
- [15] B. Shang, R. Shafin, and L. Liu, "UAV swarm-enabled aerial reconfigurable intelligent surface," *IEEE Wireless Commun.*, vol. 28, no. 5, pp. 156–163, Oct. 2021.
- [16] C. Liu, M. A. Syed, and L. Wei. "Toward ubiquitous and flexible coverage of UAV-IRS-assisted NOMA networks." Oct. 2021. [Online]. Available: <https://arxiv.org/abs/2110.04699>
- [17] T. N. Do, G. Kaddoum, L. Nguyen Thanh, D. B. da Costa, and H. Zygumt, "Aerial reconfigurable intelligent surface-aided wireless communication systems," in *Proc. IEEE Int. Symp. Pers. Ind. Mobile Radio Commun. (IEEE PIMRC)*, Oct. 2021, pp. 525–530.
- [18] T. Zhou, K. Xu, X. Xia, W. Xie, and J. Xu, "Achievable rate optimization for aerial intelligent reflecting surface-aided cell-free massive MIMO system," *IEEE Access*, vol. 9, pp. 3828–3837, Dec. 2021.
- [19] Y. Li, C. Yin, T. Do-Duy, A. Masaracchia, and T. Q. Duong, "Aerial reconfigurable intelligent surface-enabled URLLC UAV systems," *IEEE Access*, vol. 9, pp. 140248–140257, 2021.
- [20] M. T. Mamaghani and Y. Hong. "Aerial intelligent reflecting surface enabled terahertz covert communications in beyond-5G Internet of Things." Nov. 2021. [Online]. Available: <https://arxiv.org/abs/2111.11650>
- [21] H.-B. Jeon, S.-H. Park, J. Park, K. Huang, and C.-B. Chae. "An energy-efficient aerial Backhaul system with reconfigurable intelligent surface." Apr. 2021. [Online]. Available: <https://arxiv.org/abs/2104.01723>
- [22] A. Khalili, E. M. Monfard, S. Zargari, M. R. Javan, N. Mokari, and E. A. Jorswieck, "Resource management for transmit power minimization in UAV-assisted RIS HetNets supported by dual connectivity," *IEEE Trans. Wireless Commun.*, vol. 21, no. 3, pp. 1806–1822, Mar. 2022.
- [23] X. Cao *et al.*, "Reconfigurable intelligent surface-assisted aerial-terrestrial communications via multi-task learning," *IEEE J. Sel. Areas Commun.*, vol. 39, no. 10, pp. 3035–3050, Oct. 2021.
- [24] X. Mu, Y. Liu, L. Guo, J. Lin, and H. V. Poor, "Intelligent reflecting surface enhanced multi-UAV NOMA networks," *IEEE J. Sel. Areas Commun.*, vol. 39, no. 10, pp. 3051–3066, Oct. 2021.
- [25] S. Li, B. Duo, X. Yuan, Y.-C. Liang, and M. Di Renzo, "Reconfigurable intelligent surface assisted UAV communication: Joint trajectory design and passive beamforming," *IEEE Wireless Commun. Lett.*, vol. 9, no. 5, pp. 716–720, May 2020.
- [26] K. K. Nguyen, A. Masaracchia, T. Do-Duy, H. V. Poor, and T. Q. Duong. "RIS-assisted UAV communications for IoT with wireless power transfer using deep reinforcement learning." Aug. 2021. [Online]. Available: <https://arxiv.org/abs/2108.02889>
- [27] A. Al-Hilo, M. Samir, M. Elhatab, C. Assi, and S. Sharafeddine. "RIS-assisted UAV for timely data collection in IoT networks." Mar. 2021. [Online]. Available: <https://arxiv.org/abs/2103.17162>
- [28] X. Liu, Y. Liu, and Y. Chen, "Machine learning empowered trajectory and passive beamforming design in UAV-RIS wireless networks," *IEEE J. Sel. Areas Commun.*, vol. 39, no. 7, pp. 2042–2055, Jul. 2021.
- [29] K. K. Nguyen, S. Khosravirad, D. B. da Costa, L. D. Nguyen, and T. Q. Duong, "Reconfigurable intelligent surface-assisted multi-UAV networks: Efficient resource allocation with deep reinforcement learning," *IEEE J. Sel. Topics Signal Process.*, vol. 16, no. 3, pp. 358–368, Apr. 2022.
- [30] N. Agrawal, A. Bansal, K. Singh, and C.-P. Li, "Performance evaluation of RIS-assisted UAV-enabled vehicular communication system with multiple non-identical interferers," *IEEE Trans. Intell. Transp. Syst.*, early access, Nov. 2, 2021, doi: [10.1109/TITS.2021.3123072](https://doi.org/10.1109/TITS.2021.3123072).
- [31] S. Li, B. Duo, M. D. Renzo, M. Tao, and X. Yuan, "Robust secure UAV communications with the aid of reconfigurable intelligent surfaces," *IEEE Trans. Wireless Commun.*, vol. 20, no. 10, pp. 6402–6417, Oct. 2021.
- [32] Z. Ding *et al.* "A state-of-the-art survey on reconfigurable intelligent surface assisted non-orthogonal multiple access networks." 2021. [Online]. Available: [https://personalpages.manchester.ac.uk/staff/zhiguo.ding/ris\\_noma\\_proceedings.pdf](https://personalpages.manchester.ac.uk/staff/zhiguo.ding/ris_noma_proceedings.pdf)
- [33] Y. Liu *et al.* "Reconfigurable intelligent surface (RIS) aided multi-user networks: Interplay between NOMA and RIS." Oct. 2021. [Online]. Available: <https://arxiv.org/abs/2011.13336>
- [34] A. S. D. Sena *et al.*, "What role do intelligent reflecting surfaces play in multi-antenna non-orthogonal multiple access?" *IEEE Wireless Commun.*, vol. 27, no. 5, pp. 24–31, Oct. 2020.
- [35] G. Yang, X. Xu, Y.-C. Liang, and M. D. Renzo, "Reconfigurable intelligent surface-assisted non-orthogonal multiple access," *IEEE Trans. Wireless Commun.*, vol. 20, no. 5, pp. 3137–3151, May 2021.
- [36] Y. Cheng, K. H. Li, Y. Liu, K. C. Teh, and H. V. Poor, "Downlink and uplink intelligent reflecting surface aided networks: NOMA and OMA," *IEEE Trans. Wireless Commun.*, vol. 20, no. 6, pp. 3988–4000, Jun. 2021.
- [37] Z. Sun and Y. Jing, "On the performance of multi-antenna IRS-assisted NOMA networks with continuous and discrete IRS phase shifting," *IEEE Trans. Wireless Commun.*, vol. 21, no. 5, pp. 3012–3023, May 2022.
- [38] A.-T. Le, N.-D. X. Ha, D.-T. Do, A. Silva, and S. Yadav, "Enabling user grouping and fixed power allocation scheme for reconfigurable intelligent surfaces-aided wireless systems," *IEEE Access*, vol. 9, pp. 92263–92275, 2021.



- [39] Q. Chen, M. Li, X. Yang, R. Alturki, M. D. Alshehri, and F. Khan, "Impact of residual hardware impairment on the IoT secrecy performance of RIS-assisted NOMA networks," *IEEE Access*, vol. 9, pp. 42583–42592, 2021.
- [40] A. S. de Sena *et al.*, "IRS-assisted massive MIMO-NOMA networks: Exploiting wave Polarization," *IEEE Trans. Wireless Commun.*, vol. 20, no. 11, pp. 7166–7183, Nov. 2021.
- [41] T. Hou, Y. Liu, Z. Song, X. Sun, and Y. Chen, "MIMO-NOMA networks relying on reconfigurable intelligent surface: A signal cancellation-based design," *IEEE Trans. Commun.*, vol. 68, no. 11, pp. 6932–6944, Nov. 2020.
- [42] Z. Yang, Y. Liu, Y. Chen, and N. Al-Dhahir, "Machine learning for user partitioning and phase shifters design in RIS-aided NOMA networks," *IEEE Trans. Commun.*, vol. 69, no. 11, pp. 7414–7428, Nov. 2021.
- [43] X. Xu, Q. Chen, X. Mu, Y. Liu, and H. Jiang, "Graph-embedded multi-agent learning for smart reconfigurable THz MIMO-NOMA networks," *IEEE J. Sel. Areas Commun.*, vol. 40, no. 1, pp. 259–275, Jan. 2022.
- [44] R. Zhong, Y. Liu, X. Mu, Y. Chen, and L. Song, "AI empowered RIS-assisted NOMA networks: Deep learning or reinforcement learning?" *IEEE J. Sel. Areas Commun.*, vol. 40, no. 1, pp. 182–196, Jan. 2022.
- [45] H. M. Hariz, S. Sheikhzadeh, N. Mokari, M. R. Javan, B. Abbasi-Arand, and E. A. Jorswieck, "AI-based radio resource management and trajectory design for PD-NOMA communication in IRS-UAV assisted networks." Nov. 2021. [Online]. Available: <https://arxiv.org/abs/2111.03869>
- [46] X. Gao, Y. Liu, and X. Mu, "Trajectory and passive Beamforming design for IRS-aided multi-robot NOMA indoor networks," in *Proc. ICC*, Nov. 2020, pp. 1–6.
- [47] S. Jiao, X. Xie, and Z. Ding, "Deep reinforcement learning based optimization for IRS based UAV-NOMA Downlink networks." Jun. 2021. [Online]. Available: <https://arxiv.org/abs/2106.09616>
- [48] C. Huang, G. Chen, Y. Gong, M. Wen, and J. A. Chambers, "Deep reinforcement learning-based relay selection in intelligent reflecting surface assisted cooperative networks," *IEEE Wireless Commun. Lett.*, vol. 10, no. 5, pp. 1036–1040, May 2021.
- [49] X. Jia and X. Zhou, "IRS-assisted ambient backscatter communications Utilizing deep reinforcement learning," *IEEE Wireless Commun. Lett.*, vol. 10, no. 11, pp. 2374–2378, Nov. 2021.
- [50] J. Xu, X. Kang, R. Zhang, Y.-C. Liang, and S. Sun, "Optimization for master-UAV-powered auxiliary-aerial-IRS-assisted IoT networks: An option-based multi-agent hierarchical deep reinforcement learning approach." Dec. 2021. [Online]. Available: <https://arxiv.org/abs/2112.10630>
- [51] X. Gao, Y. Liu, X. Liu, and Z. Qin, "Resource allocation in IRSs aided MISO-NOMA networks: A machine learning approach," in *Proc. GLOBECOM IEEE Global Commun. Conf.*, Dec. 2020, pp. 1–6.
- [52] C. Bettstetter, H. Hartenstein, and X. Costa-Pérez, "Stochastic properties of the random waypoint mobility model," *Wireless Netw.*, vol. 10, no. 5, pp. 555–567, 2004.
- [53] A. H. Sawalmeh, N. S. Othman, H. Shakhatareh, and A. Khreishah, "Wireless coverage for mobile users in dynamic environments using UAV," *IEEE Access*, vol. 7, pp. 126376–126390, 2019.
- [54] S. M. R. Islam, N. Avazov, O. A. Dobre, and K.-S. Kwak, "Power-domain non-orthogonal multiple access (NOMA) in 5G systems: Potentials and challenges," *IEEE Commun. Surveys Tuts.*, vol. 19, no. 2, pp. 721–742, 2nd Quart., 2017.
- [55] C. Huang, A. Zappone, G. C. Alexandropoulos, M. Debbah, and C. Yuen, "Reconfigurable intelligent surfaces for energy efficiency in wireless communication," *IEEE Trans. Wireless Commun.*, vol. 18, no. 8, pp. 4157–4170, Jun. 2019.
- [56] Z. Mao, M. Peng, and X. Liu, "Channel estimation for reconfigurable intelligent surface assisted wireless communication systems in mobility scenarios," *China Commun.*, vol. 18, no. 3, pp. 29–38, Mar. 2021.
- [57] Y.-C. Liang *et al.*, "Reconfigurable intelligent surfaces for smart wireless environments: Channel estimation, system design and applications in 6G network," *Sci. China Inf. Sci.*, vol. 64, pp. 1869–1919, Jul. 2021.
- [58] Y. Pan, K. Wang, C. Pan, H. Zhu, and J. Wang, "Sum-rate Maximization for intelligent reflecting surface assisted Terahertz communications," *IEEE Trans. Veh. Technol.*, vol. 71, no. 3, pp. 3320–3325, Mar. 2022.
- [59] Z. Wan, Z. Gao, F. Gao, M. D. Renzo, and M.-S. Alouini, "Terahertz massive MIMO with holographic reconfigurable intelligent surfaces," *IEEE Trans. Commun.*, vol. 69, no. 7, pp. 4732–4750, Jul. 2021.
- [60] Z. Chen, X. Ma, C. Han, and Q. Wen, "Towards intelligent reflecting surface empowered 6G terahertz communications: A survey," *China Commun.*, vol. 18, no. 5, pp. 93–119, May 2021.
- [61] L. Xu *et al.*, "Joint location, bandwidth and power optimization for THz-enabled UAV communications," *IEEE Commun. Lett.*, vol. 25, no. 6, pp. 1984–1988, Jun. 2021.
- [62] Y. Pan, K. Wang, C. Pan, H. Zhu, and J. Wang, "UAV-assisted and intelligent reflecting surfaces-supported Terahertz communications," *IEEE Wireless Commun. Lett.*, vol. 10, no. 6, pp. 1256–1260, Jun. 2021.
- [63] Q. Pan, J. Wu, X. Zheng, W. Yang, and J. Li, "Differential privacy and IRS empowered intelligent energy harvesting for 6G Internet of Things," *IEEE Internet Things J.*, early access, Aug. 16, 2021, doi: [10.1109/JIOT.2021.3104833](https://doi.org/10.1109/JIOT.2021.3104833).
- [64] Z. Feng, B. Clerckx, and Y. Zhao, "Waveform and Beamforming design for intelligent reflecting surface aided wireless power transfer: Single-user and multi-user solutions," *IEEE Trans. Wireless Commun.*, early access, Jan. 10, 2022, doi: [10.1109/TWC.2021.3139440](https://doi.org/10.1109/TWC.2021.3139440).
- [65] M. Jian, R. Liu, and Y. Chen, "Standardization for reconfigurable intelligent surfaces: Progresses, challenges and the road ahead," in *Proc. IEEE/CIC Inter. Conf. Commun. China (ICCC Workshops)*, Jul. 2021, pp. 337–342.
- [66] R. Liu, Q. Wu, M. D. Renzo, and Y. Yuan, "A path to smart radio environments: An industrial viewpoint on reconfigurable intelligent surfaces," *IEEE Wireless Commun.*, vol. 29, no. 1, pp. 202–208, Feb. 2022.
- [67] 3GPP. "Release 17—5G enhancement for UAVs." [Online]. Available: <https://www.3gpp.org/release-17> (Accessed: Mar. 2021).

**BRENA KELLY S. LIMA** received the B.Sc. degree in computer engineering and the M.Sc. degree in electrical and computer engineering from the Federal University of Ceará, Sobral, Brazil, in 2018 and 2020, respectively. She is currently pursuing the Doctoral degree in computer science with the Universidade Lusófona de Humanidades e Tecnologias, Lisbon, Portugal. She is also a Researcher with the Cognitive and People-Centric Computing (COPELABS), where she has been working in the wireless communication field. Her research interests include mobile communications, nonorthogonal multiple access techniques, intelligent reflecting surfaces, machine learning, and unmanned aerial vehicles.

**ARTHUR SOUSA DE SENA** received the B.Sc. degree in computer engineering and the M.Sc. degree in teleinformatics engineering from the Federal University of Ceará, Brazil, in 2017 and 2019, respectively. He is currently pursuing the Doctoral degree in electrical engineering with the School of Energy Systems, LUT University, Finland. From 2014 to 2015, he studied Computer Engineering as an exchange student with the Illinois Institute of Technology, USA. He is also a Researcher with the Laboratory of Control Engineering and Digital Systems, LUT, where he has been actively working in the wireless communication field, having already published several papers in prestigious journals and conferences. His research interests include signal processing, mobile communications systems, non-orthogonal multiple access techniques, intelligent metasurfaces, and massive MIMO.

**RUI DINIS** (Senior Member, IEEE) received the Ph.D. degree from Instituto Superior Técnico (IST), Technical University of Lisbon, Portugal, in 2001, and the Habilitation degree in telecommunications from Faculdade de Ciências e Tecnologia (FCT), Universidade Nova de Lisboa (UNL) in 2010. From 2001 to 2008, he was a Professor with IST. He is currently an Associated Professor with FCT-UNL. In 2003, he was an Invited Professor with Carleton University, Ottawa, Canada. He was a Researcher with the Centro de Análise e Processamento de Sinal, IST, from 1992 to 2005 and a Researcher with the Instituto de Sistemas e Robótica from 2005 to 2008. Since 2009, he has been a Researcher with the Instituto de Telecomunicações. He has been actively involved in several national and international research projects in the broadband wireless communications area. His research interests include transmission, estimation and detection techniques. He is a VTS Distinguished Lecturer and is or was an Editor of IEEE TRANSACTIONS ON WIRELESS COMMUNICATIONS, IEEE TRANSACTIONS ON COMMUNICATIONS, IEEE TRANSACTIONS ON VEHICULAR TECHNOLOGY, IEEE OPEN JOURNAL ON COMMUNICATIONS, and *Physical Communication* (Elsevier).

**DANIEL BENEVIDES DA COSTA** (Senior Member, IEEE) was born in Fortaleza, Ceará, Brazil, in 1981. He received the B.Sc. degree in telecommunications from the Military Institute of Engineering, Rio de Janeiro, Brazil, in 2003, and the M.Sc. and Ph.D. degrees in electrical engineering, area: telecommunications from the University of Campinas, Brazil, in 2006 and 2008, respectively. His Ph.D. thesis was awarded the Best Ph.D. Thesis in Electrical Engineering by the Brazilian Ministry of Education (CAPES) at the 2009 CAPES Thesis Contest. From 2008 to 2009, he was a Postdoctoral Research Fellow with INRS-EMT, University of Quebec, Montreal, QC, Canada. From 2010 to 2022, he was with the Federal University of Ceará, Brazil. From January 2019 to April 2019, he was a Visiting Professor with the Lappeenranta University of Technology, Finland, with financial support from Nokia Foundation. He was awarded with the prestigious Nokia Visiting Professor Grant. From May 2019 to August 2019, he was with the King Abdullah University of Science and Technology, Saudi Arabia, as a Visiting Faculty, and from September 2019 to November 2019, he was a Visiting Researcher with Istanbul Medipol University, Turkey. From 2021 to 2022, he was a Full Professor with the National Yunlin University of Science and Technology, Taiwan. Since 2022, he has been with the AI & Telecom Research Center, Technology Innovation Institute, Abu Dhabi, UAE. He is an editor of several IEEE journals and has acted as symposium/track co-chair in numerous IEEE flagship conferences.

**MARKO BEKO** was born in Belgrade, Serbia, in November 1977. He received the Ph.D. degree in electrical and computer engineering from the Instituto Superior Técnico, Universidade de Lisboa, Portugal, in 2008. He received the title of a “Professor with Agregação” of electrical and computer engineering from the Universidade Nova de Lisboa, Lisbon, in 2018. His current research interests lie in the area of signal processing for wireless communications. He is the winner of the 2008 IBM Portugal Scientific Award. He serves as an Associate Editor for the IEEE OPEN JOURNAL OF THE COMMUNICATIONS SOCIETY and *Journal on Physical Communication* (Elsevier). According to the methodology proposed by Stanford University, he was among the most influential researchers in the world in 2019 and 2020 when he joined the list of top 2% of scientists whose work is most cited by other colleagues in the field of Information and Communication Technologies, sub-area Networks and Telecommunications. He is one of the founders of Koala Tech.

**RODOLFO OLIVEIRA** (Senior Member, IEEE) received the Licenciatura degree in electrical engineering from the Faculdade de Ciências e Tecnologia, Universidade Nova de Lisboa (UNL), Lisbon, Portugal, in 2000, the M.Sc. degree in electrical and computer engineering from the Instituto Superior Técnico, Technical University of Lisbon, in 2003, and the Ph.D. degree in electrical engineering from UNL in 2009. From 2007 to 2008, he was a Visiting Researcher with the University of Thessaly. From 2011 to 2012, he was a Visiting Scholar with Carnegie Mellon University. He is currently with the Department of Electrical and Computer Engineering, UNL, and is also affiliated as a Senior Researcher with the Instituto de Telecomunicações, where he researches in the areas of wireless communications, computer networks, and computer science. He serves in the Editorial Board of *Ad Hoc Networks* (Elsevier), IEEE OPEN JOURNAL OF THE COMMUNICATIONS SOCIETY, and IEEE COMMUNICATIONS LETTERS.

**MÉROUANE DEBBAH** received the M.Sc. and Ph.D. degrees from the Ecole Normale Supérieure Paris-Saclay, France. He is currently the Chief Researcher with the Technology Innovation Institute, Abu Dhabi. He is an Adjunct Professor with the Department of Machine Learning, Mohamed Bin Zayed University of Artificial Intelligence. He has managed eight EU projects and more than 24 national and international projects. His research interests include fundamental mathematics, algorithms, statistics, information, and communication sciences research. He has received more than 20 best paper awards. He is also an Associate Editor-in-Chief of *Random Matrix: Theory and Applications*. He was an Associate Area Editor and a Senior Area Editor of the IEEE TRANSACTIONS ON SIGNAL PROCESSING from 2011 to 2013 and from 2013 to 2014, respectively. Since 2021, he has been serving as an IEEE Signal Processing Society Distinguished Industry Speaker. He is a WWRF Fellow, a Eurasip Fellow, an AAIA Fellow, an Institut Louis Bachelier Fellow, and a Membre émérite SEE.